

Evaluating Treatment Prioritization Rules via Rank-Weighted Average Treatment Effects*

Steve Yadlowsky[†]

yadlowsky@google.com

Scott Fleming[†]

scottyf@stanford.edu

Nigam Shah

nigam@stanford.edu

Emma Brunskill

ebrun@cs.stanford.edu

Stefan Wager

swager@stanford.edu

November 16, 2021

Abstract

There are a number of available methods that can be used for choosing whom to prioritize treatment, including ones based on treatment effect estimation, risk scoring, and hand-crafted rules. We propose rank-weighted average treatment effect (RATE) metrics as a simple and general family of metrics for comparing treatment prioritization rules on a level playing field. RATEs are agnostic as to how the prioritization rules were derived, and only assesses them based on how well they succeed in identifying units that benefit the most from treatment. We define a family of RATE estimators and prove a central limit theorem that enables asymptotically exact inference in a wide variety of randomized and observational study settings. We provide justification for the use of bootstrapped confidence intervals and a framework for testing hypotheses about heterogeneity in treatment effectiveness correlated with the prioritization rule. Our definition of the RATE nests a number of existing metrics, including the Qini coefficient, and our analysis directly yields inference methods for these metrics. We demonstrate our approach in examples drawn from both personalized medicine and marketing. In the medical setting, using data from the SPRINT and ACCORD-BP randomized control trials, we find no significant evidence of heterogeneous treatment effects. On the other hand, in a large marketing trial, we find robust evidence of heterogeneity in the treatment effects of some digital advertising campaigns and demonstrate how RATEs can be used to compare targeting rules that prioritize estimated risk vs. those that prioritize estimated treatment benefit.

*Research partially supported by NHLBI R01 grant 5R01HL144555-02

[†]Equal contribution

1 Introduction

From medicine to marketing, algorithms are commonly used to guide decision making around personalized interventions. Some personalized intervention methods output a discrete intervention decision (often called a policy). However, the final choice of intervention for an individual is often informed both by predicted outcomes and additional considerations, such as cost or broader resource constraints. This motivates interest in other approaches that output a score that ranks individuals in terms of intervention benefit, providing a “prioritization rule” which can be used, together with other information, by decision makers in deciding a final policy. For this reason, we focus on prioritization rules in this work.

A conceptually clear approach to develop a prioritization rule is to fit a heterogeneous treatment effect model that estimates the benefit of the intervention for each individual based on their baseline covariates, and then prioritize individuals with the most intervention/treatment benefit. Recently, there have been considerable advances in methods for estimating the conditional average treatment effect (CATE) that can use data from a randomized (or appropriate observational) study to directly identify individuals most likely to benefit from an intervention (e.g., [Hill, 2011](#); [Wager and Athey, 2018](#); [Künzel et al., 2019](#)). In principle, accurately estimated CATE-based rules would be the gold standard for intervention selection and prioritization ([Manski, 2004](#)). However, learning good CATE-based rules in practice requires either running a large randomized experiment or designing a comparable quasi-experimental study, both of which involve considerable expense and effort.

A popular alternative is to first estimate the baseline probability of the outcome in absence of any intervention, and then use this as a non-causal heuristic to prioritize individuals with a high baseline risk ([Kent et al., 2020](#)). There is considerable interest in understanding the extent to which risk-based rules are sufficient for making high-quality individualized intervention decisions. For example, in medical settings, this may work well for preventative treatments where the treatment reduces the risk of an event occurring, as patients with a higher baseline risk have the most potential for benefit. In such cases, the heterogeneous treatment effect is correlated with baseline risk, but the amount of data available to build such a risk score may be much larger than that available for treatment effect estimation ([Kent et al., 2020](#)), so a risk based approach may be better. Of course, it is not always the case that the individuals with the highest risk are the ones that would benefit the most from an intervention: some customers may be very unlikely to make a purchase regardless of the ad, some patients may be too sick to benefit from a particular intervention. Therefore, it is important to validate whether a baseline risk prioritization methods is a good model for making intervention decisions.

Given this background, the purpose of this paper is to develop a suite of methods that can be used to quantify, estimate and compare the value of a treatment prioritization rule in a variety of statistical settings—including with survival endpoints subject to censoring, which are common in medical settings. Our approach is agnostic as to whether the rules were derived via CATE estimation or non-causal heuristics, and only consider the extent to which it succeeds in ranking units according to how much they benefit from the intervention. We evaluate prioritization rules via *rank-weighted average treatment effects* (RATEs), which capture the extent to which individuals who are highly ranked by the prioritization rule are more responsive to treatment than the average treatment effect. An advantage of the fact

that RATEs are agnostic to how the prioritization rule is derived is that they can be used to compare risk-based and CATE-based rules on a level playing field.

Methodologically, our paper fits into a growing literature on evaluating estimators of heterogeneous treatment effects. One of the popular metrics of this type used in the marketing literature is the Qini curve, which plots an estimate of the cumulative gain obtained by treating a growing fraction of units (as ranked by a prioritization rule) against the fraction of units treated (Radcliffe, 2007). The Qini curve is often summarized by the area under the curve, called the Qini coefficient. Recently, Imai and Li (2019) studied statistical properties of the Qini curve under randomization inference, while Sun et al. (2021) considered analogous metrics in a setting where the cost of treating units is unknown and may vary across units. Meanwhile, in the statistics literature, Zhao et al. (2013) considered a different area-under-the-curve for evaluating treatment rules. More broadly, Chernozhukov et al. (2018b) advocate assessing treatment rules by evaluating the average treatment effects across different quantiles of estimated treatment effects.

In the context of this line of work, the main contributions of our paper are as follows. First, we unify a variety of evaluation metrics under the umbrella of the RATE, including the Qini coefficient from Radcliffe (2007) and the one proposed by Zhao et al. (2013). Second, we develop estimators for the RATE that can be used in a number of statistical settings, including randomized studies and observational studies under an unconfoundedness assumption (Rosenbaum and Rubin, 1983), and that can accommodate potentially censored survival endpoints. Third, we prove a central limit theorem that applies to a wide class of RATE metrics and estimators, and that can be used to justify bootstrap-based confidence intervals. Finally, we provide empirical results on a synthetic setting, an antihypertensive treatment dataset, and an uplift marketing dataset. In this context, we discuss how different choices of RATE metrics emphasize different performance targets, which can guide selection of the right RATE metric for a given setting.

To enhance the utility of our results and methodology, we make publicly available the code used in our experiments as well as a `rank_average_treatment_effect` function provided as part of the open-source `grf` package in R. Additional materials and information are provided as part of the `grf` package documentation.

2 The Rank-Weighted Average Treatment Effect

Throughout this paper, we define causal effects in terms of the Neyman–Rubin potential outcomes model (Imbens and Rubin, 2015). We assume access to $i = 1, \dots, n$ independent and identically distributed samples $(X_i, Y_i, W_i) \in \mathcal{X} \times \mathbb{R} \times \{0, 1\}$, where W_i denotes treatment assignments, Y_i is the outcome of interest, and the X_i are auxiliary covariates. In some settings, we may need to consider a larger number of observed variables, e.g., censoring times for survival analysis; see Section 2.4 for further discussion. Following the Neyman–Rubin model, we posit potential outcomes $\{Y_i(0), Y_i(1)\}$ such that we observe $Y_i = Y_i(W_i)$, and we interpret $Y_i(1) - Y_i(0)$ as the effect of the treatment on the i -th unit. We will frequently write the conditional average treatment effect (CATE) as

$$\tau(x) = \mathbb{E} \left[Y_i(1) - Y_i(0) \mid X_i = x \right]. \quad (1)$$

Given this notation, we're ready to formalize the main building blocks of our analysis, namely a prioritization rule and its associated targeting operator characteristic curve, which characterizing how different the average treatment effect (ATE) is in units above each quantile of the prioritization rule from the ATE in the entire population.

Definition 1. A prioritization rule is defined in terms of a priority scoring function $S : \mathcal{X} \rightarrow \mathbb{R}$, such that samples $i = 1, \dots, n$ are prioritized in order $j = 1, \dots, n$ for treatment in decreasing order of $S(X_i)$ (that is, a larger value of $S(X_i)$ implies that the sample should be treated first). We let $i(j)$ denote the mapping from the rank j to the sample index i .

Remark 1. Throughout our analysis, we treat the priority scoring function $S(\cdot)$ as fixed and deterministic; our n samples will only be used to evaluate $S(\cdot)$ (i.e., they act as a test set). In practice, $S(\cdot)$ could either be taken from a published resource, or $S(\cdot)$ could be learned from an auxiliary dataset. In the latter case, our results on estimation and inference should be understood as conditional on $S(\cdot)$.

Let $F_S(\cdot)$ be the cumulative distribution function (CDF) of $S(X_i)$. For now, we will assume that there are no ties in the prioritization rule S , so that F_S is continuous; see Section 2.3 for a discussion of a randomized tiebreaking scheme for when there are ties.

Definition 2. For any rule with priority score $S(\cdot)$ and any threshold $0 < u \leq 1$ such that $F_S^{-1}(u)$ exists, the targeting operator characteristic (TOC) is

$$\text{TOC}(u; S) := \mathbb{E} \left[Y_i(1) - Y_i(0) \mid F_S(S(X_i)) \geq 1 - u \right] - \mathbb{E} [Y_i(1) - Y_i(0)]. \quad (2)$$

Note if $u = 1$, the first term is the average treatment effect, and so $\text{TOC}(u; S) = 0$.

Our main proposal involves evaluating prioritization rules in terms of weighted averages of the TOC, which we refer to as rank-weighted average treatment effects (RATEs). We emphasize that the RATE only depends on the priority score $S(\cdot)$ via its induced priority ranking, and not via the numeric values of $S(X_i)$ for individual units. After defining the RATE, we show below that a number of evaluation metrics considered in the literature are in fact special cases of a RATE.

Definition 3. For any weight function $\alpha : (0, 1] \rightarrow \mathbb{R}$, the induced rank-weighted average treatment effect (RATE) of a priority score $S(\cdot)$ is

$$\theta_\alpha(S) = \int_0^1 \alpha(u) \text{TOC}(u; S) du. \quad (3)$$

Remark 2. In order to validate the claim that the RATE measures the ability of a prioritization rule to effectively target treatment, consider the following sanity checks. If the priority score $S(\cdot)$ is not predictive of the individual treatment effects $Y_i(1) - Y_i(0)$, i.e., $S(X_i) \perp\!\!\!\perp Y_i(1) - Y_i(0)$, then we immediately see that both the TOC and any RATE will be identically 0. Furthermore, if a priority score is monotone predictive of treatment effects in the sense that $f(s) = \mathbb{E}[Y_i(1) - Y_i(0) \mid S(X_i) = s]$ is non-decreasing in s , then $\text{TOC}(u; S)$ is non-negative and non-increasing for $u \in (0, 1)$, and any RATE with non-negative weighting function will be non-negative.

Example 1 (high-vs-others). A very simple way to assess the effectiveness of a prioritization rule is by comparing the ATE for the top u -th of units prioritized by the rule to the overall ATE. This “high versus others” comparison metric is a RATE, with weight function corresponding to a point mass at u and $\theta(S) = \text{TOC}(u; S)$.

Example 2 (AUTOC). One limitation of the high-vs-other metric is that it is focused on comparisons at a specific quantile $F_S^{-1}(u)$ that needs to be selected. One natural way to avoid this difficulty and to get a quantile-agnostic performance measure is to consider the area under the TOC curve, $\text{AUTOC}(S) = \int_0^1 \text{TOC}(u; S) du$. This metric was also considered in [Zhao et al. \(2013\)](#).

Example 3 (Qini). The Qini coefficient is another possible “under the curve” metric. The Qini curve ([Radcliffe, 2007](#)) is defined by evaluating cumulative benefits as we increase the treatment fraction according to a prioritization rule, and the Qini coefficient measures the area under the Qini curve:

$$\text{QINI}(S) = \int_0^1 \mathbb{E} \left[1 \left(\{F_S(S(X_i)) \geq 1 - u\} \right) (Y_i(1) - Y_i(0)) \right] - u \mathbb{E} [Y_i(1) - Y_i(0)] du. \quad (4)$$

This is a RATE with linear weight function $\alpha(u) = u$, i.e., $\text{QINI}(S) = \int_0^1 u \text{TOC}(u; S) du$.

Example 4 (AUPEC). [Imai and Li \(2019\)](#) proposed a modified Qini-coefficient, which they call the AUPEC rule. The AUPEC chooses a threshold s^* such that no units are assigned to treatment if the priority score falls below s^* :

$$\begin{aligned} \text{AUPEC}(S; s^*) = \int_0^1 \mathbb{E} \left[1 \left(\{F_S(S(X_i)) \geq \max \{1 - u, F_S(s^*)\}\} \right) (Y_i(1) - Y_i(0)) \right] \\ - u \mathbb{E} [Y_i(1) - Y_i(0)] du. \end{aligned} \quad (5)$$

The AUPEC with score threshold $s^* \neq 0$ is not a RATE, because it also depends on the value of $S(X_i)$ as opposed to the induced ranking only.

2.1 Weighted ATE Representation

Interestingly, we can represent RATEs (3) as a weighted average of the individual treatment effects $Y_i(1) - Y_i(0)$, with weights depending on the quantile of $S(X_i)$. For any weight function $\alpha(u)$ for a RATE metric as in Definition 3, define

$$w_a(t) = \int_t^1 \frac{\alpha(u)}{u} du - \int_0^1 \alpha(u) du, \quad (6)$$

assuming that these integrals exist and are finite. Proposition 3 shows that $\theta_\alpha(S)$ has a natural representation as an average treatment effect weighted by w_α .

Proposition 3. *Let $\alpha(u)$ be the weight function for a RATE metric as in Definition 3. Assume that $\mathbb{E} [Y_i(1) - Y_i(0) | X_i = x]$ is uniformly bounded. If $\alpha(u)$ is absolutely integrable on $[0, 1]$ and $\alpha(u)/u$ is absolutely integrable on $[t, 0]$ for any $t \in (0, 1)$, then $\theta_\alpha(S)$ can be written equivalently as*

$$\theta_a(S) = \mathbb{E} \left[w_a (1 - F_S(S(X_i))) (Y_i(1) - Y_i(0)) \right]. \quad (7)$$

This representation is valuable for a number of reasons. First, from Proposition 3, we immediately see that all the RATE metrics considered above have the following representations:

$$\begin{aligned}\text{TOC}(u; S) &= \mathbb{E} \left[\left(\left(1 \{ F_S(S(X_i)) \geq 1 - u \} / u \right) - 1 \right) (Y_i(1) - Y_i(0)) \right], \\ \text{AUTOC}(S) &= \mathbb{E} \left[\left(-\log(1 - F_S(S(X_i))) - 1 \right) (Y_i(1) - Y_i(0)) \right], \\ \text{QINI}(S) &= \mathbb{E} \left[(F_S(S(X_i)) - 1) (Y_i(1) - Y_i(0)) \right].\end{aligned}\tag{8}$$

This gives further insight into the qualitative behavior of different RATE metrics. For example, we see that the AUTOC measure strongly upweights treatment effects for the very first units prioritized by $S(\cdot)$ (i.e., with $F_S(S(X_i)) \approx 1$), whereas the Qini coefficient considers the beginning and end of the ranking given by $S(X_i)$ symmetrically.

Second, the representation (7) provides a natural starting point for a unified asymptotic analysis of RATE metrics. As we will see in Section 3, it is most convenient to state regularity assumptions and prove results for statistics of the form (9). This representation enables us to leverage a large and well understood set of asymptotics results for L -statistics (Shorack and Wellner, 2009).¹ We can then apply these results to RATE metrics via Proposition 3.

This representation gives us an alternative way to define a RATE. For any $w : (0, 1) \rightarrow \mathbb{R}$ that satisfies appropriate regularity conditions on w (a formal discussion is presented in the Supplementary Materials), any centered weighted ATE of the form

$$\eta_w(S) = \mathbb{E} \left[w(1 - F_S(S(X_i))) (Y_i(1) - Y_i(0)) \right]\tag{9}$$

is also a RATE. By centered, we mean that $\int_0^1 w(u) du = 0$. Then, we have that the weighted ATE in (9) is equivalent to a RATE metric as defined in Definition 3 with weights $\alpha_w(\cdot)$ defined as follows,

$$\eta_w(S) = \theta_{\alpha_w}(S), \quad \alpha_w(t) = -tw'(1 - t).\tag{10}$$

2.2 Estimating the RATE

Our goal is to provide a general framework for designing estimators for RATEs that can be applied in a wide variety of statistical settings, including observational studies and studies with survival endpoints. To this end, we follow the approach used by Semenova and Chernozhukov (2017) and Athey and Wager (2021) to design flexible methods for estimating the best linear predictor of the treatment effect and policy learning, respectively, under similar generality. The main idea is to assume the existence of “scores” $\widehat{\Gamma}_i$ with the property that they act as nearly unbiased (but noisy) proxies for the CATE (1),

$$\mathbb{E} \left[\widehat{\Gamma}_i \mid X_i \right] \approx \tau(X_i) = \mathbb{E} \left[Y_i(1) - Y_i(0) \mid X_i \right].\tag{11}$$

¹Strictly speaking, η_w as defined in (9) is not an L -statistic because of the random multiplicative factor $Y_i(1) - Y_i(0)$. However, this will not impede our application of standard results on L -statistics in proving a central limit theorem.

The law of iterated expectation means that we can replace $Y_i(1) - Y_i(0)$ with such a score in definition of the TOC (2) and weighted ATE representation of RATEs (9), as long as the approximation in (11) is good. In the case of evaluating the effect of a treatment on non-survival outcomes in a randomized controlled trial with randomization probability π , one simple choice of scoring rule we could use is inverse-propensity weighting, i.e.,

$$\widehat{\Gamma}_i = \frac{W_i Y_i}{\pi} - \frac{(1 - W_i) Y_i}{1 - \pi}. \quad (12)$$

In this case (11) holds exactly. In general, however, constructing scores $\widehat{\Gamma}_i$ in more complicated settings (including with survival outcomes) requires more care and involves estimation of nuisance components (Chernozhukov et al., 2016). We defer a discussion of how to construct scores $\widehat{\Gamma}_i$ and precise conditions of the type (11) to Section 2.4, and for now take the availability of such scores as given.

Given this setting, we estimate the TOC and RATE by sample-averaging estimators. First, for any $1/n \leq q \leq 1$, we estimate the TOC as

$$\widehat{\text{TOC}}(u; s) = \frac{1}{\lfloor un \rfloor} \sum_{j=1}^{\lfloor un \rfloor} \widehat{\Gamma}_{i(j)} - \frac{1}{n} \sum_{i=1}^n \widehat{\Gamma}_i. \quad (13)$$

This TOC estimator also induces a natural RATE estimator that can be applied with smooth weight functions $\alpha(\cdot)$:

$$\widehat{\theta}_\alpha(S) = \frac{1}{n} \sum_{j=1}^n \alpha\left(\frac{j}{n}\right) \widehat{\text{TOC}}\left(\frac{j}{n}; S\right). \quad (14)$$

The weighted ATE representation in (7) induces a natural estimator that does not require $\alpha(\cdot)$ to be smooth. In this form, we can use $\widehat{\Gamma}_i$ directly in the empirical estimate

$$\widehat{\eta}_{w_\alpha}(S) = \frac{1}{n} \sum_{i=1}^n w\left(\frac{j}{n}\right) \widehat{\Gamma}_{i(j)}. \quad (15)$$

2.3 Tiebreaking

So far, we have assumed that the priority score $S(\cdot)$ provides a strict priority ranking. In many settings of interest, however, $S(\cdot)$ may have ties. In these cases, we break ties by considering all possible permutations of orderings within each set of tied observations, and then averaging the resulting TOC estimates. Thus, in the presence of ties, our definition of the TOC from (2) generalizes to

$$\begin{aligned} \text{TOC}(u; S) &= \frac{P(S(X_i) > q_u)}{u} \mathbb{E} \left[Y_i(1) - Y_i(0) \mid S(X_i) > q_u \right] \\ &+ \left(1 - \frac{P(S(X_i) > q_u)}{u}\right) \mathbb{E} \left[1 \left(\{S(X_i) = q_u\} \right) (Y_i(1) - Y_i(0)) \right] \\ &- \mathbb{E} [Y_i(1) - Y_i(0)], \end{aligned} \quad (16)$$

where $q_u = \sup\{q : F_S(q) \leq u\}$. Notice that when there are no ties, so that $P(S(X_i) > q_u) = u$, this simplifies to the previous expression for the TOC. Similarly, the sample-average TOC

estimator (13) averages the $\widehat{\Gamma}_i$ across tied observations: If $S(X_{i(k)}) > S(X_{i(k+1)}) = \dots = S(X_{i(k')})$ for some $k < m < k'$, then

$$\widehat{\text{TOC}}\left(\frac{m}{n}; s\right) = \frac{1}{m} \left(\sum_{j=1}^k \widehat{\Gamma}_{i(j)} + \frac{m-k}{k'-k} \sum_{j=k+1}^{k'} \widehat{\Gamma}_{i(j)} \right) - \frac{1}{n} \sum_{i=1}^n \widehat{\Gamma}_i. \quad (17)$$

Given these these tie-robust definitions of the TOC, our definition (3) of the RATE and as associated estimator (14) remain as is.

The weighted ATE representation in (7) can also be adapted by taking the average of the weights over all possible tie-breaking orders. That is, by replacing $w(t)$ at any t with $P(S(X_i) = t) = v > 0$ with its average over the ties,

$$\frac{1}{v} \int_0^v w(F_S(t) - \epsilon) d\epsilon.$$

Similarly, for the empirical estimate, by replacing $w(m/n)$ at any $k < m < k'$ with $S(X_m) = S(X_{k'})$ with

$$\frac{1}{k'-k} \sum_{j=k+1}^{k'} w(j/n).$$

2.4 Score construction

One advantage of the RATEs, and their estimators discussed in Section 2.2, is their generality in terms of causal estimation strategies. To re-iterate, the key to estimation is deriving a score $\widehat{\Gamma}_i$ that approximately satisfies Eq. (11). Because individual treatment effects depend on unobserved counterfactuals, construction of such a score remains nontrivial. Here, we provide a summary of some useful scores from a variety of causal estimation strategies.

Many of the scores derived below depend on quantities that must be estimated, motivating the use of the hat $\widehat{\cdot}$ in $\widehat{\Gamma}_i$. These quantities are not inherently of interest, except that they allow construction of such a score; therefore, we shall refer to them as nuisance parameters. It's useful to compare these scores to an *oracle* score where the nuisance parameters are known a priori, which we denote Γ_i^* . The oracle score will usually satisfy the condition (11) exactly,

$$\mathbb{E} \left[\Gamma_i^* \mid X_i \right] = \tau(X_i).$$

Then, we can quantify the score estimation error that results from the fact that we must estimate the nuisance parameters as

$$\delta_i := \widehat{\Gamma}_i - \Gamma_i^*. \quad (18)$$

The score estimation error δ_i will be useful for studying the RATE estimation error and inference in Section 3.

Randomized Trials As mentioned in Section 2.2, randomized trials admit a simple IPW score that satisfy the condition (11) exactly, given in Eq. (12). The exact unbiasedness of this score is appealing, however, it can be high variance.

Using an Augmented IPW (AIPW) estimator can help reduce the variance by adjusting for the baseline covariates X_i measured at the beginning of the trial,

$$\begin{aligned}\widehat{\Gamma}_i &= \hat{m}(X_i, 1) - \hat{m}(X_i, 0) + \frac{W_i - \pi}{\pi(1 - \pi)} (Y_i - \hat{m}(X_i, W_i)), \\ \hat{m}(x, w) &\approx \mathbb{E}[Y_i(w)|X_i = x]\end{aligned}\tag{19}$$

where the nuisance parameter $m(x, w)$ represents the expected outcome given a subject's covariates and treatment assignment $w \in \{0, 1\}$. The nuisance parameter is not known in practice, and therefore must be estimated—either using an appropriate parametric model, a nonparametric / machine learning estimator, or a simple surrogate such as the lagged outcome at the time of randomization.

Because in a randomized trial, the treated proportion π is known, so that $\mathbb{E}[W_i | X_i] = \pi$, the estimated score $\widehat{\Gamma}_i$ from (19) satisfies the condition (11) exactly whenever $\hat{m}(\cdot, \cdot)$ is independent of the i -th example, either because it is fixed or estimated on an independent fold of data.

Observational Study with Unconfoundedness In this context, we estimate doubly robust scores for each participant using AIPW scores [Robins et al. \(1994\)](#):

$$\widehat{\Gamma}_i = \hat{m}(X_i, 1) - \hat{m}(X_i, 0) + \frac{W_i - \hat{e}(X_i)}{\hat{e}(X_i)(1 - \hat{e}(X_i))} (Y_i - \hat{m}(X_i, W_i)),\tag{20}$$

$$e(x) = P[W_i = 1 | X_i = x], \quad m(x, w) = \mathbb{E}[Y_i(w)|X_i = x]\tag{21}$$

where $e(x)$ represents the probability of an individual being assigned to treatment conditioned on observables; $m(x, w)$ represents the expected outcome given a subject's covariates and treatment assignment $w \in \{0, 1\}$; and $\hat{e}(x)$, $\hat{m}(x, w)$ represent nonparametric estimates of $e(x)$ and $m(x, w)$, respectively.

The oracle score would be

$$\Gamma_i^* = m(X_i, 1) - m(X_i, 0) + \frac{W_i - e(X_i)}{e(X_i)(1 - e(X_i))} (Y_i - m(X_i, W_i)).$$

This satisfies the condition (11) exactly, because $\mathbb{E}[Y_i - m(X_i, W_i) | X_i, W_i] = 0$, and $\tau(X_i) = m(X_i, 1) - m(X_i, 0)$.

The scores for randomized trials can be thought of as a simplified version of the scores for observational studies, where the propensity score is known $e(X_i) = \pi$. This removes the estimation error, leading to the estimated scores exactly satisfying condition (11) for randomized trials, but only approximately satisfying this condition for observational studies.

Time-to-event Outcomes The AIPW approach for both randomized trials and observational studies can be generalized to handle time-to-event outcomes with right-censored

outcomes. To do so, we first need to introduce some additional notation to specify the event times and censoring times. We denote the counterfactual event times as $T_i(1)$ and $T_i(0)$, and the counterfactual censoring times as $C_i(1)$ and $C_i(0)$. With censored data, we only observe the factual event time $T_i = T_i(W_i)$ up to the factual censoring time $C_i = C_i(W_i)$. That is, the observed data are $U_i = \min\{T_i, C_i\}$ and $\Delta_i = 1\{U_i = T_i\}$.

Two endpoints that are often used with time-to-event outcomes can be easily adapted to the methods developed here. To study absolute risk, we use the outcome

$$Y_i(w) = 1\{T_i(w) \leq t_0\},$$

and to study the restricted mean survival time, we use

$$Y_i(w) = \min\{T_i(w), t_0\},$$

for a pre-specified time t_0 that denotes the end of observation. The causal effect estimated in each case is the absolute risk reduction

$$P\left(T_i(1) \leq t_0 \mid X_i = x\right) - P\left(T_i(0) \leq t_0 \mid X = x\right),$$

and the difference in restricted mean survival time,

$$\mathbb{E}\left[\min\{T_i(1), t_0\} - \min\{T_i(0), t_0\} \mid X = x\right].$$

With either of these endpoints, we use the augmented IPW approach described in [Tsiatis \(2007\)](#), based off of the construction from [Robins et al. \(1994\)](#), and used as a score for CATE estimation in [Cui et al. \(2020\)](#). For either of these endpoints, the score is the same. Let $\tilde{U}_i = \min\{U_i, t_0\}$, $\tilde{\Delta}_i = 1\{U_i = T_i \text{ or } C_i > t_0\}$ and $Y_i = Y_i(W_i)$ as defined above for each endpoint. Then, the score is

$$\begin{aligned} \hat{\Gamma}_i &= \hat{m}(X_i, 1) - \hat{m}(X_i, 0) + \frac{W_i - \hat{e}(X_i)}{(1 - \hat{e}(X_i))\hat{e}(X_i)} \left(\frac{\tilde{\Delta}_i Y_i - (1 - \tilde{\Delta}_i) \hat{q}(\tilde{U}_i, X_i, W_i)}{\hat{S}_C(\tilde{U}_i, X_i, W_i)} \right. \\ &\quad \left. - \int_0^{\tilde{U}_i} \frac{\hat{q}(s, X_i, W_i)}{\hat{S}_C(s, X_i, W_i)} d\hat{\Lambda}_C(s, X_i, W_i) - \hat{m}(X_i, W_i) \right), \end{aligned} \quad (22)$$

with

$$\begin{aligned} m(x, w) &= \mathbb{E}\left[Y_i \mid X_i = x, W_i = w\right], \\ q(u, x, w) &= \mathbb{E}\left[Y_i \mid X_i = x, U_i \geq u, W_i = w\right], \text{ and} \\ S_C(s, x, w) &= P(C_i \geq s \mid X_i = x, W_i = w). \end{aligned}$$

Similarly to the observational study setting, \hat{e} , \hat{m} , \hat{q} , and \hat{S}_C refer to nonparametrically estimated versions of the corresponding functions defined without a $\hat{\cdot}$. The oracle score Γ_i^* is the equivalent with all of the estimated functions replaced with their corresponding true function.

Cross-fitting All of the scores defined in this section require estimation of an unknown nuisance parameter function, which we will generically denote as $\eta(v)$, where v is some generic set of arguments to the nuisance parameter. For example, for observational studies, $m(x, w)$ and $e(x)$ are unknown, and must be estimated.

One issue that can occur when estimating these nuisance parameters and then plugging them in to the score equation is that the nuisance parameters estimated depend on the same observations that they are applied to in the score equation. When using machine learning approaches to estimate the nuisance parameters, this can lead to the difference δ_i between the estimated scores and oracle scores being too large, violating the assumptions needed for convergence discussed in Section 3.

To avoid this, we can split the sample into two components, one for estimating the nuisance parameters, and the other for applying the score functions. However, we would then only have score estimates for a fraction of the observations. By splitting the data into k folds, and repeating the sample splitting estimates of the nuisance parameters on each fold, we can avoid the inter-dependence between the scores and nuisance parameter estimates while still getting an estimated score for every observation. This technique, called cross-fitting, is discussed extensively in Chernozhukov et al. (2018a). Using cross-fitting with the scores discussed in this section and appropriate machine learning estimators of the nuisance parameters will achieve the needed assumptions on δ_i in Assumption C that we will introduce in Section 3.

3 Asymptotics and Inference

In order for the RATE to be a useful tool for assessing priority scoring rules, we need to be able to use RATE estimates as the basis for hypothesis tests for comparing different scoring rules. In this section, we will provide a central limit theorem for a large family of RATE estimators that will enable confidence intervals and hypothesis tests via bootstrap-based methods. Throughout this section, we will assume for simplicity that that $S(X_i)$ has no ties; however, all our results extend immediately to the case with ties via the randomized tiebreaking procedure discussed in Section 2.3.

In Sections 2.1 and 2.2, we discussed two representations for the RATE and its estimator, respectively. Except for technical issues related to regularity conditions, the representations of the RATE in Section 2.1 are equivalent (see Prop. 3, and Eq. 10). It is most convenient to state regularity assumptions and prove results for statistics of the weighted ATE form (9). On the other hand, the estimators (14) and (15) are similar in spirit, but not precisely equivalent. However, both can be represented in the following generalized form of (15),

$$\hat{\theta} = \frac{1}{n} \sum_{j=1}^n w_n \left(\frac{j}{n} \right) \hat{\Gamma}_{i(j)}, \quad (23)$$

where w_n is now a sequence of empirical weight functions that depends on the sample size n . As long as w_n converges to w , in an appropriate sense discussed below, any estimator of the form (23) will have similar statistical behavior to the exact plug-in estimator (15).

3.1 A Central Limit Theorem

The realizable estimator $\widehat{\theta}$ is asymptotically linear under certain conditions on the data generating distribution, the weight function of the metric, and the nuisance parameter estimates used to construct $\widehat{\Gamma}_i$. We derive the asymptotic variance of the estimator. We then discuss how this enables construction of confidence intervals and an asymptotically valid hypothesis test using the bootstrap.

For notational convenience throughout this section, we will use $Q = S(X)$ and $Q_i = S(X_i)$.

Assumption A. *There are almost surely no ties in the scores $S(X)$, so that $F_S(s)$ is continuous. The weights w_n and w are asymptotically similar, and each is sufficiently diffuse: w and w_n are both squared integrable on $(0, 1)$, and there exists $M < \infty$ and $b < 1$ satisfying the conditions of Assumption B and Assumption C, so that $|w(t)| \leq B(t) := M(t(1-t))^{-b}$ for $b < 1$,*

$$\mathbb{E} \left[\frac{1}{n} \sum_{j=1}^n \left(w_n(j/n) - w(1 - F_S(Q_{i(j)})) \right)^2 \right] \rightarrow 0,$$

and

$$\limsup_{n \rightarrow \infty} \sum_{j=1}^n \left(w_n(j/n) - w(j/n) \right)^p < \infty \text{ for some } p > 2.$$

Assumption B. *There exists $C_g < \infty$ such that $\text{Var}(\Gamma_i^* \mid X_i = x) \leq C_g$. $\bar{\tau}(q)$ is of bounded variation. $\mathbb{E}[|\bar{\tau}(Q)|^r] < \infty$ for some $r > 2$ satisfying $1/r + b < 1/2$ and $1/r \leq 1 - 1/p$ with b and p defined in Assumption A.*

To satisfy the variance condition for the IPW or AIPW score, a sufficient condition is that there exists $C_v < \infty$ such that $\sigma_w^2(x) := \text{Var}(Y(w) \mid X = x) \leq C_v$ and $\text{Var}(Y(w)) \leq C_v$, and there exists $0 < C_e < \infty$ such that $C_e \leq P(W = 1 \mid X = x) \leq 1 - C_e$.

Assumption C. *(a) The δ_i are (uniformly) randomly partitioned into $K \in \mathbb{N}$ (independently of n) sets $\{I_k\}_{k=1}^K$, each containing n/K items, with $\{\delta_i\}_{i \in S_k}$ independent, conditionally on $B_k = \{(Y_i, W_i, X_i)\}_{i \notin I_k}$ and an event G_k with $P(G_k) \rightarrow 1$. (b) The bias $\mathbb{E}[\sqrt{n}w(1 - F_S(Q_i))\delta_i \mid G_k, B_k] \rightarrow 0$, and $q \mapsto \mathbb{E}[w(1 - F_S(Q_i))\delta_i \mid Q_i = q, G_k, B_k]$ is of bounded variation. (c) The higher moments of δ_i satisfy $\mathbb{E}[(1 + B^2(F(Q_i))(t(1-t))^\epsilon)\delta_i^2 \mid Q_i = q, G_k, B_k] \leq \max\{\zeta_n v(q), C\}$ with $\epsilon > 0$, $\mathbb{E}[v(Q_i)] < \infty$, $\zeta_n \rightarrow 0$ and $C < \infty$, and finally $\mathbb{E}[\delta_i^r] < \infty$ for r satisfying the same conditions as in Assumption B.*

This assumption is satisfied if (i) the IPW score is used with a known propensity score (such as in a randomized experiment), or (ii) the AIPW score is used with nuisance parameters that are known or estimated with cross-fitting (Chernozhukov et al., 2018a) satisfying $\|\widehat{\pi}(\cdot) - \pi(\cdot)\|_{m,P} \max\{\|\widehat{\mu}_1(\cdot) - \mu_1(\cdot)\|_{m,P}, \|\widehat{\mu}_1(\cdot) - \mu_1(\cdot)\|_{m,P}\} = o_P(n^{-1/2})$, and $\|\widehat{\pi}(\cdot) - 1/2\|_{\infty,P} > 0$. The norm m is often 2 (eg., if $w(\cdot)$ is bounded), but may require $m > 2$ if the weight function w heavily upweights certain regions of Q . Part (a) is a sufficient condition to allow the approximation error terms to be uncorrelated within each partition by allowing one to condition on the nuisance parameters fit using cross-fitting, although it can be generalized so long as $\text{Cov}(\delta_i, \delta_j \mid G_k, B_k) = o(1/n)$ for $i, j \in I_k$. This allows generalization to

leave-one-out cross-fitting schemes under sufficiently regular nuisance parameter estimation methods.

With these assumptions, we can give our main result, showing that the estimated RATE metric is asymptotically linear (and therefore, asymptotically normal) under these assumptions.

Theorem 4. *Under Assumptions A-C,*

$$\sqrt{n}(\hat{\theta} - \theta) = \frac{1}{\sqrt{n}} \sum_{i=1}^n \psi_i + o_P(1),$$

with $\psi_i = w(1 - F_S(S(X_i)))(\Gamma_i^* - \bar{\tau}(S(X_i))) + \int_{S(X_i)}^\infty w(1 - F_S(q)) d\bar{\tau}(q) - \theta$.

There are two key ideas in Theorem 4. The first is quantifying the variation that comes from weighting observations by estimated quantiles of the prioritization rule instead of the true quantiles. This we connect to the theory of L -statistics (van der Vaart, 1998; Shorack and Wellner, 2009), by noticing that

$$\frac{1}{n} \sum_{j=1}^n w_n \left(\frac{j}{n} \right) \bar{\tau}(S(X_{i(j)})),$$

with $\bar{\tau}(q) = \mathbb{E}[Y_i(1) - Y_i(0) \mid S(X_i) = q]$ is an L -statistic. Then, the second is the use of the scores $\hat{\Gamma}_i$ in place of $\bar{\tau}(Q_i)$ in the estimator $\hat{\theta}$. Such scores are helpful for estimating any parameter that is a linear functional of $\tau(X_i)$. By the law of iterated expectations, the same is true for linear functionals of $\bar{\tau}(Q_i)$, so long as the weights only depend on Q_i . The representation of RATEs in the weighted ATE form show that RATEs satisfy this requirement. The approach for replacing $\tau(X_i)$ with $\hat{\Gamma}_i$ has been used for average treatment effect estimation (Chernozhukov et al., 2018a), conditional average treatment effect estimation (Kennedy, 2020), policy learning (Athey and Wager, 2021), and structural functions of treatment effects (Semenova and Chernozhukov, 2017). The key to proving Theorem 4 (done in Section 8) is extending this technique to L -statistics.

Asymptotic linearity with an influence function with finite variance implies the validity of a wide variety of inference methods, such as many bootstrap resampling methods for inference (Mammen, 2012). Typical proofs require stronger conditions, such as requiring the estimator to be a Hadamard differentiable functional of the empirical distribution function (van der Vaart, 1998). These would impose extra conditions on the weight function for RATE metrics beyond the assumptions we require for Theorem 4. However, the half-sample bootstrap requires only asymptotic linearity,² and therefore is a justified method for inference on any RATE metric under the assumptions of Theorem 4. Let $\hat{\theta}^*$ be the estimate using a random sample (without replacement) of $n/2$ of the observations. The following corollary of Theorem 4 justifies that the distribution over the selection of samples to include in the half-sample estimate converges to the sampling distribution of $\hat{\theta}$ (see Section A.2.1 in the Supplementary Materials for proof).

²This is shown in Lemma 12 of the Supplementary Materials, although the method has a long history in the statistics literature (Kish and Frankel, 1970; Efron, 1982).

Corollary 5. *Under the assumptions of Theorem 4, let V be the asymptotic distribution of $\sqrt{n}(\hat{\theta} - \theta)$. Let $\hat{\theta}^*$ be an estimate of a RATE using a random sample (without replacement) of $n/2$ of the observations. Under the same assumptions as Theorem 4,*

$$\sqrt{n}(\hat{\theta}^* - \hat{\theta}) \xrightarrow{d} V,$$

conditionally on $(X_i, Y_i, W_i)_{i=1}^n$.

From these results, we get a few corollaries justifying the asymptotic linearity of, and bootstrapped inference for, the previously proposed evaluation metrics. First, we show that any weight function $w : [0, 1] \rightarrow \mathbb{R}^+$ that is squared-integrable and uniformly continuous satisfies the assumptions on the weight function from Theorem 4.

Lemma 6. *Assume that $w : [0, 1] \rightarrow \mathbb{R}^+$ is squared-integrable and uniformly continuous on its range, $[0, 1]$. Then, $E[\frac{1}{n} \sum_{j=1}^n (w(j/n) - w(1 - F_S(S(X_{i(j)})))^2] \rightarrow 0$.*

See Section A.2.2 in the Supplementary Materials for proof. This immediately implies the following corollary for the Qini score.

Corollary 7. *The Qini coefficient, for completely randomized trials as initially described in Radcliffe (2007), or for observational data satisfying the no unobserved confounding assumption using the AIPW score, is \sqrt{n} -consistent and asymptotically linear, as long as the data satisfies Assumption B and the nuisance parameter estimates satisfy Assumption C.*

The weight function for the AUTOC is not uniformly continuous. Nonetheless, it still satisfies Assumption A, according to the following proposition, also proved in Section A.2.3.

Proposition 8. *The weight function $w_n(t) = H_n - H_{\lfloor nt \rfloor + 1} - 1$ for the AUTOC satisfies the conditions of Assumption A with $w(t) = -\log(t) - 1$. Therefore, above estimator of the AUTOC is \sqrt{n} -consistent and asymptotically linear, as long as the data satisfies Assumption B and the nuisance parameter estimates satisfy Assumption C with any $r > 2$.*

3.2 Hypothesis Testing and Confidence Intervals

An important aspect of RATE metrics is that they provide a natural null hypothesis for testing whether a prioritization rule is useful for identifying subpopulations with heterogeneous treatment effects. Consider the null hypothesis $H_0: \theta_\alpha(S) \leq 0$. The hypothesis test H_0 described above is sensitive to treatment effect heterogeneity aligned with the prioritization rule S .

Additionally, a test of H_0 can be interpreted as a test of treatment effect heterogeneity. If there is no treatment effect heterogeneity, meaning that $\tau(X) = \tau$ is constant, then $\text{TOC}(u; S) = 0$ for any $u \in (0, 1]$, and so $\theta_\alpha(S) = 0$. However, it will not be a powerful test for treatment effect heterogeneity without a good prioritization rule. The statistic $\theta_\alpha(S)$ can be zero if there is no treatment effect heterogeneity, or if the prioritization rule S has no relationship with the heterogeneous treatment effects. Some may find it advantageous, that instead of simply testing whether heterogeneous treatment effects exist, it tests whether the treatment effect is predictable by some prioritization rule. However, those interested in

studying whether heterogeneous treatment effects exist regardless of whether or not they can be identified by a prioritization rule should consider tests such as Ding et al. (2016).

Using the sampling distribution for $\hat{\theta}$ from Section 3.1, we can easily develop a valid test for H_0 using the bootstrap. Let σ^* denote the standard deviation of the bootstrap estimates $\hat{\theta}^*$. Then, an asymptotically valid P -value for H_0 is

$$2\Phi\left(-\frac{|\hat{\theta}|}{\sigma^*}\right),$$

where Φ is the CDF of the unit normal distribution, $\mathbf{N}(0, 1)$. Similarly, we can use the sampling distribution to derive asymptotically valid confidence intervals for $\theta_\alpha(S)$. To get a $1 - \alpha$ confidence interval, we can use

$$\hat{\theta} \pm z_{1-\alpha/2}\sigma^*,$$

where $z_{1-\alpha/2} = \Phi^{-1}(1 - \alpha/2)$, and, as above, σ^* is the standard deviation of the bootstrap estimates $\hat{\theta}^*$.

4 Comparing the Power of Qini vs. AUTOC

An important question regarding RATE metrics concerns which weighting function one should use. We try to shed light on this question through a set of simple but illustrative experiments. Overall, we conclude that the RATE metric with the best signal-to-noise ratio (and thus power for testing whether the RATE for a given prioritization rule is different from 0) depends on how the treatment effects differ across quantiles of the prioritization rule. To illustrate this, we construct simulations representing scenarios in which almost all subjects exhibit a linearly varying CATE, as well as scenarios in which only a small portion of the population experiences a varying CATE, and some in between.

We draw $n = 400$ samples from a standard uniform distribution $X_i \sim \text{Unif}(0, 1)$, then let the marginal response under treatment, $\mu_1(X_i)$, marginal response under control, $\mu_0(X_i)$, potential outcomes under treatment and control, $Y_i(1)$ and $Y_i(0)$ respectively, and treatment effect for each individual, $\tau(X_i)$, be given as follows:

$$\mu_0(x) = 0 \tag{24}$$

$$\mu_1(x) = \max\left(-\frac{2}{p^2}x + \frac{2}{p}, 0\right) \tag{25}$$

$$Y_i(0) = \mu_0(X_i) + \varepsilon_i \tag{26}$$

$$Y_i(1) = \mu_1(X_i) + \varepsilon_i \tag{27}$$

$$\tau(x) = \mathbb{E}\left[Y_i(1) - Y_i(0) \mid X_i = x\right] = \mu_1(x) - \mu_0(x) \tag{28}$$

where $\varepsilon \sim \mathbf{N}(0, 0.2)$ represents i.i.d. random noise and p is a simulation-specific parameter representing the proportion of individuals for whom the CATE is non-zero. We consider a simple prioritization rule $S(X_i) = 1 - X_i$. This prioritization rule is “perfect” in the sense that, for all x_i and x_j in $[0, 1]$, $S(x_i) > S(x_j)$ implies $\tau(x_i) > \tau(x_j)$. When $p = 1.0$, the CATE

is nonzero (and varying linearly over quantiles of the prioritization rule). When $p = 0.1$, only a small subset of the population has a nonzero CATE, but the treatment effect is large and changing quickly with the quantile.

Using this setup, we both the AUTOC and Qini metrics, and repeat this procedure 10000 times for each p in $\{1.0, 0.5, 0.1\}$. Figure 1 shows the distribution of the estimates of each metric over these 10000 Monte Carlo simulations. We note that, given some fixed sample size, n , the variance of the weights applied to each doubly robust score in the AUTOC is constrained to be 1 while the variance of the weights applied to these same scores for the Qini coefficient tends toward 0.5 for large n .³ We thus rescaled the Qini coefficient weights to also have variance 1 for the purposes of this analysis, in order to fairly compare the two metrics. While this rescaling changes the value of the point estimate for these methods, it does not change the statistical power of the two approaches.

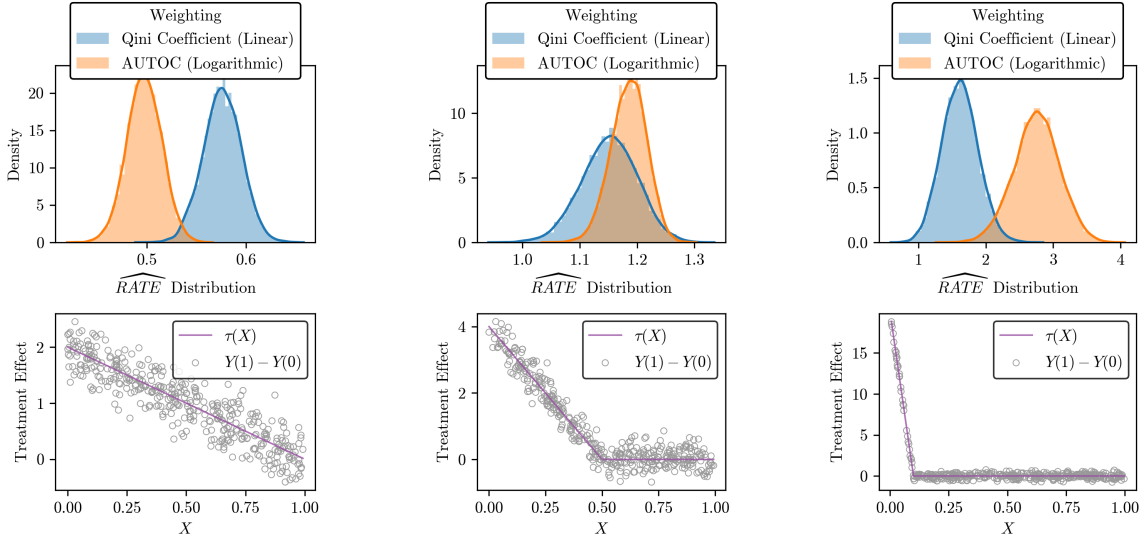
When all or a substantial portion (e.g., $> 50\%$) of the treatment effects are both heterogeneous and non-zero, using the Qini metric can lead to a higher RATE compared to the AUTOC. However, when only a small subset of individuals have a non-zero heterogeneous treatment effect (e.g., $\leq 10\%$), using AUTOC can lead to a higher RATE and thus be advantageous. Although hardly comprehensive, this small example highlights a broader intuition about when and why one might choose linear weighting vs. logarithmic weighting in estimating the RATE: If a researcher believes that only a small subset of their study population experiences nontrivial heterogeneous treatment effects, they should use logarithmic weighting; if they believe that heterogeneous treatment effects are diffuse and substantial across the entire study population, they should use linear weighting. Following this guideline should, in general, increase the statistical power of tests against the absence of heterogeneous treatment effects.

5 Prioritization Rules for Antihypertensive Treatment

Hypertension, or elevated blood pressure (BP), is the leading risk factor for overall burden of disease worldwide (Fisher and Curfman, 2018; Lim et al., 2012), and was implicated in 14% of all deaths across the globe in 2015 (Qamar and Braunwald, 2018). Furthermore, hypertension has a high prevalence in both the United States ($\geq 45\%$ (Muntner et al., 2018)) and other countries (e.g., $\geq 50\%$ in China and Japan (Khera et al., 2018; Feitosa et al., 2018)). It is the greatest risk factor for cardiovascular death in every major region of the world (Gakidou et al., 2017). A high systolic BP (SBP) substantially increases one's risk of developing a stroke, myocardial infarction, heart failure, and other adverse cardiovascular events (Fisher and Curfman, 2018).

Evidence suggests that effective treatment of hypertension can, in many instances, significantly reduce the risk of negative cardiovascular disease outcomes (Psaty et al., 1997; Pahor et al., 2000; Psaty et al., 2003). However, while lowering an individual's BP is thought to reduce cardiovascular risk in general, it is less clear the degree to which benefits of intensively targeting a low BP with antihypertensive medications are uniform across patients. Antihypertensives are also associated with serious risks and adverse side effects (Group, 2010,

³This limit can be calculated by computing the integral for variance of the weights in the representation in Eq. (8), with the helpful observation that $F_S(Q_i)$ is uniform on $(0, 1)$.



(a) 100% have $|\tau(X_i)| > 0$ (b) 50% have $|\tau(X_i)| > 0$ (c) 10% have $|\tau(X_i)h| > 0$

Figure 1. Comparison of linear (Qini) vs. logarithmic (AUTOC) weighting functions. If treatment effects are nonzero for a significant proportion of the population (e.g., left figure) the power of the estimated RATE when using linear weighting (Qini) tends to be greater than when using logarithmic (AUTOC) weighting. Conversely, if nonzero treatment effects are concentrated among a small proportion of the population (e.g., right figure) we see that using logarithmic (AUTOC) weighting leads to a greater power for the estimated RATE relative to using linear (Qini) weighting.

2015), such that most guidelines account for individualized targets in the elderly based on frailty (Qaseem et al., 2017; Unger et al., 2020). Thus, developing personalized treatment rules based on individualized benefit is of interest to doctors and patients alike.

One common way to determine who should be targeted for antihypertensive medications is via risk-based targeting, motivated by a hypothesis that patients with at the highest a priori risk for heart disease should also be most likely to net benefit from the medication. The advantage of risk-based targeting is that there are well-established estimates of 10-year cardiovascular disease risk in patients age 40 years or older, including the Framingham Risk Score (D'Agostino et al., 2008) and the ASCVD Risk Estimator (Goff et al., 2014), that are readily available for clinicians and can thus immediately be used as a prioritization rule for the appropriate populations. For example, the the American College of Cardiology and American Heart Association 2017 guidelines recommend that, in patients with Stage 1 hypertension (SBP of 130-139 mm Hg), antihypertensive medications should be used for intensive blood pressure targeting only if the estimated 10-year CVD risk is $\geq 10\%$, as measured by the ASCVD Risk Estimator (Whelton et al., 2018; Goff et al., 2014). In 2021, guidance was updated to suggest that low-risk adults with stage 1 hypertension should start medical therapy if they do not lower BP with lifestyle modifications after 3-6 months (Jones et al., 2021).

We study personalized treatment rules for hypertension in the context of two large randomized controlled trials on the effectiveness of intensive blood-pressure control: the Systolic

Blood Pressure Intervention Trial (SPRINT) (Group, 2015) and the Action to Control Cardiovascular Risk in Diabetes Blood Pressure trial (ACCORD-BP) (Group, 2010). The overall finding of SPRINT was that intensive BP control (i.e., titrating antihypertensives to decrease a patient’s SBP to a target of < 120 mm Hg) is more effective than standard therapy (i.e., targeting < 140 mm Hg) in reducing the risk of major cardiovascular events, at least among the trial population considered (older adults with an elevated baseline cardiovascular risk). However, the effectiveness found in ACCORD-BP was much lower, which may be due to differences in the BP titration procedure (Huang et al., 2017), or differences between the populations studied in the two trials (Beddhu et al., 2018; Basu et al., 2017; Kaul, 2017).

Prior work has been motivated by the hypothesis that differences between the overall treatment effect in SPRINT and ACCORD could be explained by heterogeneity in treatment effect (Huang et al., 2017; Kaul, 2017). For example, Beddhu et al. (2018) suggested that in ACCORD, intensive BP management was more effective at reducing CVD and death under standard glycemia control than under intensive glycemia control. Basu et al. (2017) reported that despite the overall treatment effect not generalizing well from SPRINT to ACCORD-BP, treatment heterogeneity estimated via interaction terms in a Cox model did have some evidence of doing so. Duan et al. (2019) found that the treatment effect in deciles of the CATE estimated using a machine learning model showed a better trend towards treatment effectiveness than the ASCVD Risk Estimator, although the error bars in each decile were large. Since these papers were published, causal survival forests (Cui et al., 2020), a new method for CATE estimation with survival data, has been published.

Our overall strategy will be to estimate RATE metrics for a number of prioritization rules on both ACCORD-BP and SPRINT.⁴ We develop a CATE model using causal survival forests, and using the methodology developed here for RATEs, we formally test the hypotheses that (a) this new CATE model finds treatment effect heterogeneity, and (b) that the estimated treatment heterogeneity is better correlated with treatment effectiveness than estimates from risk models.

5.1 ACCORD-BP and SPRINT

Conducted in 2001-2005 and 2010-2013, respectively, the ACCORD-BP and SPRINT trials share many similarities, most notably the treatment tested (intensive vs. standard blood-pressure control, as defined above) and secondary outcomes of interest (myocardial infarction, stroke, heart failure, death from cardiovascular causes, and all-cause mortality). The two trials also have several important differences. In terms of trial design, the ACCORD BP trial was conducted on 4733 participants with type 2 diabetes, while SPRINT was conducted on 9361 participants at high risk for cardiovascular disease, but without diabetes. Differences in age-based inclusion criteria also led to a slightly younger trial population in ACCORD-BP (mean age, 62 years) relative to SPRINT (mean age, 68 years). The primary outcome considered in the ACCORD-BP trial was a composite outcome of myocardial infarction, stroke, or death from cardiovascular causes, while the SPRINT trial’s primary composite outcome consisted of the above as well as other acute coronary syndromes and heart failure.

⁴All data access was performed by Stanford-affiliated co-authors, Google did not have access to the data. The analyses conducted with de-identified patient data were approved by the institutional panel on human subjects research at Stanford School of Medicine under protocol 46829.

The original focus of both the ACCORD-BP and SPRINT trials was to assess the overall benefit of intensive blood-pressure treatment. From this perspective, the ACCORD-BP trial found that patients assigned to the intensive blood-pressure treatment arm had a 12% (95% CI, -6% to 27%) lower risk of the primary composite outcome relative to the standard blood-pressure control arm. Meanwhile the SPRINT trial found that individuals in the intensive blood-pressure treatment arm had a 25% (95% CI, 11% to 36%) lower risk relative to controls; and in fact the SPRINT trial was terminated early because the benefits of intensive blood pressure control for the population in consideration became clear before the predetermined study endpoint.

5.2 Prioritization Rules

When considering standard pre-specified prioritization rules, i.e., in our case, the Framingham Risk Score and the ASCVD Risk Estimator, priority scoring functions $S(\cdot)$ are already available and so we can proceed directly. Meanwhile, when considering CATE-based methods as well as other risk-based alternatives, we need to learn a prioritization rule before being able to evaluate it. In order to avoid overfitting to idiosyncrasies of any given experiment, we always learn prioritization rules on the other dataset than the one used for evaluation: Specifically, any prioritization rules evaluated on ACCORD-BP are learned from SPRINT, and vice-versa.

In both SPRINT and ACCORD-BP, we estimate the RATE metric for each of five prioritization rules — some well-established risk-based prioritization rules, and some data-driven prioritization rules that directly target the CATE — and use confidence intervals for the RATE to test against the presence of heterogeneous treatment effects in these two trials. For these 6 different prioritization rules (Causal Survival Forest, Cox Proportional Hazards S-learner, Random Forest Risk model, the Framingham Risk Score, the ASCVD Risk Estimator), we (1) estimate optimal parameters of the prioritization rule on one trial; then (2) estimate a 95% bootstrapped confidence interval for the RATE using 10,000 bootstrapped samples from patient data in the other trial; and (3) calculate the P -value of a two-sided test of the null hypothesis that the RATE is zero as described in Section 3.2.

We describe a number of relevant prioritization rules for survival outcomes in Section B.2.2 of the Supplementary Materials. Here, we briefly describe a few more that are relevant to this problem in particular:

Framingham Risk Score The global Framingham risk score equations to predict cardiovascular disease (FRS) are well-established models that predict an individual's 10-year risk of developing atherosclerotic cardiovascular disease (ASCVD) in patients without a prior cardiac event (D'Agostino et al., 2008; D'Agostino Sr et al., 2013). The FRS tool consists of two separate multivariate models: one for males and one for females. Each model takes as input a patient's age, sex, current smoking status, systolic blood pressure, diabetes diagnosis, and whether the patient is currently being treated with medications to reduce their blood pressure. Multiple studies have validated the ability of the Framingham Risk Score to discriminate between high- and low-risk patients (Bozorgmanesh et al., 2011; Artigao-Rodenas et al., 2013; Carroll et al., 2014), though its moderate to poor calibration in such studies — particularly among younger patients, women, and ethnically diverse cohorts — has been criticized (DeFilippis et al., 2015; Cook et al., 2012; Sionis et al., 2012).

Prioritization Rule	AUTOC (95% CI)	<i>p</i> -value
Causal Survival Forest (grf)	1.64 (-4.05, 7.34)	0.59
Cox PH S-learner	4.27 (-2.05, 10.59)	0.13
Random Survival Forest Risk (grf)	3.47 (-3.55, 10.49)	0.39
Framingham Risk Score	2.48 (-2.83, 7.80)	0.40
ACC/AHA Pooled Cohort Equations	2.11 (-4.23, 8.45)	0.50

Table 1. AUTOC estimates obtained using data from SPRINT ($n = 9069$), with scoring rules trained on ACCORD-BP ($n = 4535$) if necessary. We also show 95% confidence intervals obtained via the procedure outlined in Section 3.2, along with associated *p*-values.

ACC/AHA Pooled Cohort Equations In an effort to improve the FRS, the ACC/AHA Pooled Cohort Equations (PCEs) uses a set of risk estimates from pooling cohorts to map a patient’s risk factors to a 10-year risk of developing atherosclerotic cardiovascular disease (ASCVD) (Goff et al., 2014). Similar to the construction of the FRS, the PCEs consists of four separate multivariate models, stratified by race (White and Black) and sex (men and women). In addition to the variables measured by the FRS, the PCEs also incorporates information about patients’ race and diabetes status into its estimates. As with the FRS, the PCEs have been well-validated as a tool for predicting patients’ 10-year risk of developing ASCVD, though their performance on certain population subgroups has similarly been criticized (Yadlowsky et al., 2018).

5.3 Results

See Table 1 for results from training prioritization rules on ACCORD-BP and evaluating them on SPRINT, and Table 2 for results from training prioritization rules on SPRINT and evaluating them on ACCORD-BP.

In this experiment, the estimated RATE for every risk-based prioritization rule (Random Survival Forest, FRS, and ACC/AHA PCEs) was not significantly different from zero when evaluated on both ACCORD-BP and SPRINT. These findings suggest that, for these two trial populations, the risk-based estimators in consideration would not order patients in accordance with estimated treatment benefit. Additionally, the estimated RATE prioritization rules that directly target the CATE (the Causal Survival Forest and Cox Proportional Hazards S-Learner) were not significantly different from 0 in both ACCORD-BP and SPRINT, using confidence level $\alpha = 0.05$ with *P*-values generated via the procedure outlined in Section 3.2.

5.4 Discussion and Limitations

Our findings show no significant evidence of heterogeneous treatment effects in the SPRINT and ACCORD-BP trials.⁵ This suggests that the variables included in our analysis were insufficient to distinguish those individuals who were most likely to benefit from those who

⁵Note the average treatment effect over all subjects in the trials may have been significant, as suggested in the original SPRINT trial results.

Prioritization Rule	AUTOC (95% CI)	<i>p</i> -value
Causal Survival Forest (grf)	-3.6 (-15.32, 8.12)	0.55
Cox PH S-learner	8.58 (-3.21, 20.38)	0.16
Random Survival Forest Risk (grf)	1.35 (-9.99, 12.69)	0.83
Framingham Risk Score	5.51 (-1.60, 12.62)	0.13
ACC/AHA Pooled Cohort Equations	-3.32 (-13.21, 6.57)	0.48

Table 2. AUTOC estimates obtained using data from ACCORD-BP ($n = 4535$), with scoring rules trained on SPRINT ($n = 9069$) if necessary. We also show 95% confidence intervals obtained via the procedure outlined in Section 3.2, along with associated *P*-values.

were least likely to benefit. This could be because there is in fact no significant heterogeneity in treatment effect in the two trials. It could also be attributable to insufficient sample size, though we note that these two trials are large in comparison to other trials of similar complexity. From the results on these data, it remains ambiguous whether or not clinical use of risk scores like the Framingham Risk Score or ACC/AHA Poole Cohort Equations to guide patients towards intensive blood pressure control regimens is in fact more beneficial than simply using the original trial’s inclusion/exclusion protocols to ensure alignment between the trial cohort population and the patient population to which the trial’s evidence is subsequently applied. The RATE, however, provides a principled approach for evaluating whether such prioritization rules should be used to guide clinical care at all.

We note that our findings using RATE on SPRINT and ACCORD-BP disagree with some of the earlier findings of significant heterogeneous treatment effects in these trials reported by Basu et al. (2017) and Duan et al. (2019). In correspondence with the authors, we discovered subtle issues in methodology and/or reporting that would tend to invalidate some of those prior findings of heterogeneous treatment effects in these trials. We think this highlights the benefit of using the RATE as a tool for formal, rigorous inspection and testing of hypotheses around treatment heterogeneity.

6 Prioritization Rules for Uplift Modeling

Personalized treatment effect estimation has attracted considerable attention from the marketing literature, under the name *uplift modeling* (Radcliffe, 2007; Ascarza, 2018). Estimators of the CATE can be used for selection or prioritization of individuals for marketing campaigns (Radcliffe and Surry, 1999; Radcliffe, 2007) or customers for interventions to increase retention (Ascarza, 2018). In both cases, uplift modeling approaches are a response to more classical approaches based on prioritizing individuals based on the probability of conversion or churn, respectively.

More broadly, marketers appreciate that the treatment effect of marketing campaigns is the best measure of a campaign’s effectiveness (Hohnhold et al., 2015; Johnson et al., 2017). Indeed randomized trials (A/B experiments) are widely used to evaluate marketing campaigns (Radcliffe, 2007; Gordon et al., 2019). Randomized trials are particularly easy to design and implement in the world of digital marketing, and many tools exist to help data scientists run these experiments (Gordon et al., 2019).

One challenge in defining a treatment effect for a marketing campaign as a contrast

	Full data		Training subsample		Test subsample	
	Visit	Conversion	Visit	Conversion	Visit	Conversion
Treatment	0.0485	0.0031	0.0492	0.0031	0.0488	0.0031
Control	0.0382	0.0019	0.0395	0.0019	0.0377	0.0021

Table 3. Visit and conversion rates in each arm of the Criteo Uplift Benchmark dataset, and our two randomly subsampled datasets for training and testing uplift models. Tests for difference in means between the rates of the three samples are insignificant at 5%-level.

between a treatment and control is to define what the control should be. In the case of email or paper mail campaigns, the treatment might simply be sending a potential customer mail and the control might be sending the customer nothing. However, for online digital advertising, there are a number of different causal effects that might be of interest. For example, one might be interested in comparing bidding on an ad location versus not, or whether a user was shown your ad versus a competitor’s ad (Johnson et al., 2017). Choosing the right causal effect, and designing the appropriate study for measuring that effect is important, and we will assume that such a decision has already been made.

6.1 Criteo Uplift Benchmark

Criteo released a large benchmark dataset for studying uplift modeling in online digital advertising, based on anonymized results from a number of incrementality trials (Diemert et al., 2018). In combining trials, the interpretation of the treatment is subtle, corresponding to an intent to treat with one of a handful of arbitrarily chosen ads. The purpose of the data is to provide a benchmark for uplift modeling, and therefore, the results are not meant to be used in a particular application. See Diemert et al. (2018) for more information about the dataset construction and validation.

For the purposes of anonymization, the features released are a random projection of the user features into a 12-dimensional space. The data also contain a binary indicator for treatment status, and two outcomes, visiting the site following the ad, and further conversion into a customer. The data contain 25,309,483 samples with an unbalanced fraction of treated vs control units; however, we randomly selected two sets of 320,000 samples without replacement, each equally balanced with 160,000 treated and 160,000 control units. We used the first set for training prioritization rule models, and the second set for evaluating the RATE metrics of the learned models.

Diemert et al. (2018) reports that the combined trials had an average visit rate of 0.04132 and an average conversion rate of 0.00229. They report a relative average treatment effect of 68.7% increase on the visit rate and 37.2% increase on the conversion rate, however the data have been updated to fix some biases found in combining multiple trials. The average visit and conversion rates in the treatment and control arms of the updated dataset and our subsamples are reported in Table 3. They correspond to relative average treatment effects of a 27.0% increase in visit rates and a 59.4% increase in conversion rates in the full data, which are similar in the subsamples.

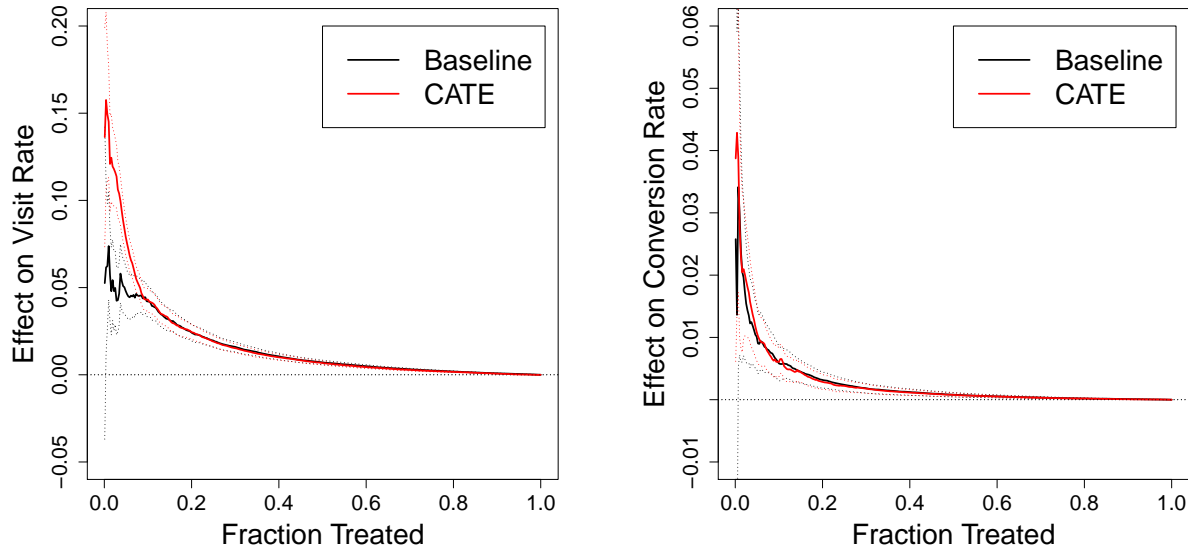


Figure 2. TOC curves for two prioritization rules (baseline- and CATE-based) and two outcomes (rate of visits and rate of conversion) on Criteo Uplift benchmark dataset.

6.2 Prioritization Rules

We considered two random-forest based prioritization rules, one fit to the baseline probability of the outcome if untreated (ie., how likely is the user to visit or convert without any advertising), and one fit using causal forests for the conditional average treatment effect. We will call these the baseline and CATE prioritization rules, respectively. In both cases, we used default hyperparameters, except for the minimum node size and `mtry` parameter. The smaller the minimum node size, the slower that fitting the random forests becomes, and this is particularly problematic for the large dataset size used here. We selected the minimum node size to be 5000, which was the smallest value such that the forest could be fit reasonably quickly on a modern laptop computer. We selected the optimal `mtry` parameter for both algorithms with respect to the AUTOCC on the test dataset. Because there are only 12 possible values for this parameter, and because the test set is large, the bias in the final results introduced by doing this is negligible.

6.3 Results

Figure 2 shows the TOC curves for each of the prioritization rules for each of the outcomes, and Table 4 shows the RATE metrics (AUTOC and Qini coefficient) summarizing these curves, along with their confidence intervals.

Both methods on both outcomes work better than random prioritization, with strictly positive CIs. For visits, the AUTOCC for the CATE-based prioritization rule is marginally higher than the baseline-based rule; the difference between their AUTOCC statistics is 0.0036 (95% CI 0.0020, 0.0053), which is a relative increase in AUTOCC of 25%. However, the Qini coefficient and the results for conversions are not significantly different between the two prioritization rules. Looking at the TOC curves in Figure 2 gives suggestions as to why

	AUTOC (95% CI)		Qini coefficient (95% CI)	
	Visit	Conversion	Visit	Conversion
Baseline	0.0136 (0.0111, 0.0161)	0.0023 (0.0011, 0.0035)	0.0059 (0.0048, 0.0069)	0.00074 (0.00047, 0.00101)
CATE	0.0171 (0.0148, 0.0194)	0.0025 (0.0015, 0.0035)	0.0058 (0.0049, 0.0067)	0.00070 (0.00044, 0.00096)

Table 4. RATE metrics on Criteo Uplift Benchmark dataset. Confidence intervals are estimated using bootstrapped standard errors as described in Section 3.2.

this is the case. From these curves, we can see that the average treatment effect among the highest prioritized individuals according to the CATE-based rule is much higher than for the baseline-based rule at similar fractions treated. However, the difference disappears once the fraction treated is more than 10%. The Qini coefficient weights the TOC by the fraction treated, so it downweights the importance of these small groups with large treatment benefit. On the other hand, these groups are more influential in the AUTOC, explaining why we observe a statistically significant difference in this metric. Note that while the confidence intervals overlap between the two metrics, the correlation between them, due to the fact that the estimates come from the same test set, means that the confidence intervals for the contrast of RATE metrics or TOC curves are much smaller.

6.4 Discussion and Limitations

Our goal here was not to build an optimal prioritization rule, but to demonstrate how RATE metrics can be used to find heterogeneity and compare treatment prioritization rules. The results in this section give robust evidence in favor of the presence of treatment effect heterogeneity in the treatment effects of some digital advertising campaigns. Our methodology for developing the prioritization rules was intentionally kept simple, for reproducibility purposes. By using a larger subset of the data, trying models that take longer to train, and more carefully tuning the hyperparameters, one may be able to improve the prioritization rules more.

Additionally, the exact treatment applied in the Criteo Uplift Benchmark is unknown, and the features are anonymized, preventing external validation of the prioritization rules obtained. The presence of heterogeneity in these data do not ensure that all marketing campaigns have substantial heterogeneity, although they do suggest that in some cases, looking for heterogeneity may be promising. Additionally, they suggest that the AUTOC is a better summarization metric of the TOC curve, that is more sensitive to differences between prioritization rules' ability to select small groups with large treatment effects, which appear to be important in these data.

7 Discussion

In this work, we discuss evaluation of treatment prioritization rules with an emphasis on the downstream impact on outcomes. In a similar spirit to the immensely popular Area under the Receiver-operating Characteristic curve (AUROC) (Green et al., 1966; Zweig and

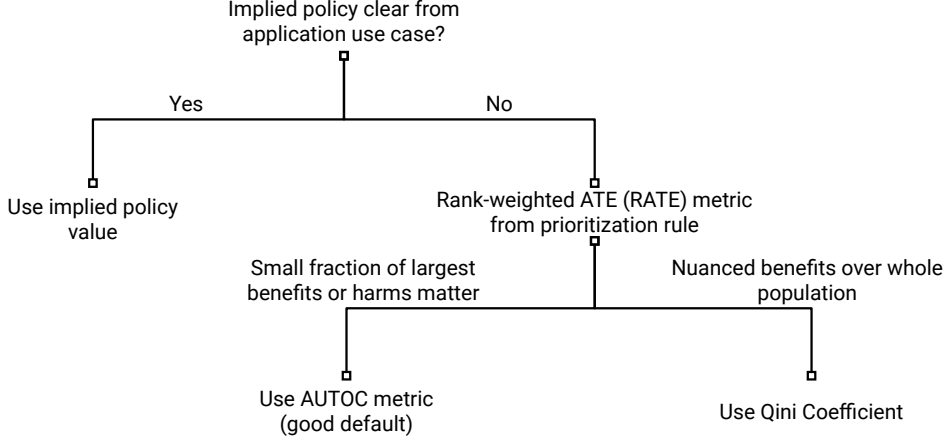


Figure 3: A flowchart for choosing the best evaluation metric to use in an application.

[Campbell, 1993](#)), our proposed evaluation approach using the RATE enables policy- and decision threshold-agnostic evaluation and comparison of risk-based and CATE-based estimators alike. Researchers can use the RATE and the procedure outlined in Section 3.2 to (1) evaluate whether a single prioritization rule performs significantly better than chance/random treatment allocation in stratifying subjects according to estimated treatment benefit; (2) directly, meaningfully, and rigorously compare the targeting performance of two different prioritization rules and determine whether one exhibits significant superiority; and (3) perform a global test for the presence of predictable heterogeneous treatment effects, by coupling estimation of the RATE with a powerful, flexible, non-parametric CATE estimator as the prioritization rule (i.e., the Causal Forest or Causal Survival Forest as illustrated in Sections 5 and 6). We show in Section B.3 that such tests can be performed with high statistical power, even with reasonably small sample sizes and relatively low signal-to-noise ratios. Our approach works in the context of both continuous, real-valued outcomes and right-censored, time-to-event outcomes, making it a practical tool for a number of different fields of study, from marketing and business to medicine and public policy.

To apply a treatment prioritization rule in practice, one must convert the prioritization rule into a policy for whom to intervene on versus not. From this perspective, it's intuitive to consider directly evaluating the prioritization rule on the average reward of the policy implied by thresholding the prioritization rule at a specified level. If the details of how the prioritization rule will be converted into a policy—e.g. treat with antihypertensive medications with 10-year risk of ASCVD $\geq 10\%$ —are known at the time of evaluation, this is a reasonable approach.

However, in many cases, the policy is unclear or may still be subject to change at the time that the prioritization rule is designed. For instance, in healthcare applications, the policy for final treatment decisions might additionally depend on individualized risk of serious adverse events from the treatment, patient and provider preferences, costs, and other considerations. In marketing applications, they may depend on varying costs associated with advertising, concerns for advertisement blindness ([Hohnhold et al., 2015](#)) and other considerations.

RATE metrics provide a way to summarize the quality of a treatment prioritization rule

in ranking units according to potential without specifying a particular treatment policy. This can be especially beneficial when evaluating the degree to which risk-based and other non-centered targeting algorithms optimize treatment benefit.

Choosing the appropriate RATE metric for a problem can be important. As noted in Section 4, the precision (and thus, statistical power) of a RATE metric depends on the weighting scheme and the shape of the true, underlying TOC curve. In applications where a data scientist anticipates that the prioritization rule will be used to find a relatively small group of individuals with a large treatment benefit, they should use the AUTOC curve; the digital advertising example in Section 6 illustrates the practical impacts here. However, in cases where treatment effects are more evenly spread out over the population, the Qini coefficient might be more powerful. From our experience so far working with these metrics, we recommend starting with the AUTOC metric if one is unsure which would be more appropriate. We summarize the above discussions of how to choose an effective metric for heterogeneous treatment effects in applications as a flowchart in Figure 3.

8 Proof of Main Results

8.1 Proof of Proposition 3

Proof Let $A = \int_0^1 \alpha(u) du$. Now, note that

$$\begin{aligned}\theta_a(S) &= \int_0^1 \alpha(u) \mathbb{E} \left[Y_i(1) - Y_i(0) \mid F_S(S(X_i)) \geq 1 - u \right] du - A \mathbb{E} [Y_i(1) - Y_i(0)] \\ &= \int_0^1 \frac{\alpha(u)}{u} \mathbb{E} \left[(Y_i(1) - Y_i(0)) \mathbf{1} \left(\{F_S(S(X_i)) \geq 1 - u\} \right) \right] du - A \mathbb{E} [Y_i(1) - Y_i(0)] \\ &= \int_0^1 \frac{\alpha(u)}{u} \mathbb{E} \left[\tau(X_i) \mathbf{1} \left(\{F_S(S(X_i)) \geq 1 - u\} \right) \right] du - A \mathbb{E} [Y_i(1) - Y_i(0)].\end{aligned}$$

By recalling that we assumed $\tau(X)$ is uniformly bounded and $\frac{\alpha(u)}{u}$ is absolutely integrable on $1 \geq u \geq 1 - F_S(S(X_i))$ for almost every $S(X_i)$, we can apply Fubini's Theorem to get

$$\begin{aligned}&= \mathbb{E} \left[(Y_i(1) - Y_i(0)) \int_0^1 \frac{\alpha(u)}{u} \mathbf{1} \left(\{F_S(S(X_i)) \geq 1 - u\} \right) du \right] - A \mathbb{E} [Y_i(1) - Y_i(0)] \\ &= \mathbb{E} \left[(Y_i(1) - Y_i(0)) \int_{1-F_S(S(X_i))}^1 \frac{\alpha(u)}{u} du \right] - A \mathbb{E} [Y_i(1) - Y_i(0)].\end{aligned}$$

□

8.2 Proof of Theorem 4

Proof Let $\widehat{F}_S(q^-)$ denote the empirical distribution at the left limit, instead of the right, and define $\widehat{G}_S(q) = 1 - \widehat{F}_S(q^-)$, which is the empirical distribution function of the observations in the reverse order. Note that the quantile j/n of the $i(j)$ -th example is simply

$\widehat{G}_S(Q_{i(j)})$. Then, we decompose $\sqrt{n}(\widehat{\theta} - \theta)$ into two leading terms that we show are asymptotically linear, followed by remainder terms that we show vanish under Assumptions A-C.

$$\begin{aligned}
\frac{1}{\sqrt{n}} \sum_{i=1}^n w_n(\widehat{G}_S(Q_i)) \widehat{\Gamma}_i - \theta &= \underbrace{\frac{1}{\sqrt{n}} \sum_{i=1}^n w(1 - F_S(Q_i))(\Gamma_i^* - \bar{\tau}(Q_i))}_{\text{Term 1}} \\
&\quad + \underbrace{\frac{1}{\sqrt{n}} \sum_{i=1}^n w(\widehat{G}_S(Q_i))\bar{\tau}(Q_i) - \theta}_{\text{Term 2}} \\
&\quad + \underbrace{\frac{1}{\sqrt{n}} \sum_{i=1}^n (w_n(\widehat{G}_S(Q_i)) - w(\widehat{G}_S(Q_i)))\bar{\tau}(Q_i)}_{\text{Term 3}} \\
&\quad + \underbrace{\frac{1}{\sqrt{n}} \sum_{i=1}^n (w_n(\widehat{G}_S(Q_i)) - w(1 - F_S(Q_i)))(\Gamma_i^* - \bar{\tau}(Q_i))}_{\text{Term 4}} \\
&\quad + \underbrace{\frac{1}{\sqrt{n}} \sum_{i=1}^n w_n(\widehat{G}_S(Q_i))\delta_i}_{\text{Term 5}}
\end{aligned}$$

Term 1

The first term is trivially a sum of iid random variables.

Term 2

The second term (which we will denote as T_n) is an L -statistic (van der Vaart, 1998; Shorack and Wellner, 2009) with $\bar{\tau}(q)$ of bounded variation. To show that it is asymptotically linear, we use the following assumptions and theorem from Shorack and Wellner (2009):

Assumption D. [Assumption 1, Shorack and Wellner (2009)] (a) The weight function $w : (0, 1) \rightarrow \mathbb{R}$ satisfies $|w(1-t)| \leq B(t) = Mt^{-b_1}(1-t)^{-b_2}$ for $M < \infty$ and $\max\{b_1, b_2\} < 1$, and (b) $\bar{\tau}(q) = \bar{\tau}_+(q) - \bar{\tau}_-(q)$, each monotone non-decreasing, with $|\bar{\tau}_\pm(F_S^{-1}(t))| \leq D(t) = Mt^{-d_1}(1-t)^{-d_2}$.

Assumption E. [Assumption 2', Shorack and Wellner (2009)] (a) w has a continuous derivative on $(0, 1)$ satisfying $|w'(1-t)| \leq \frac{B(t)}{t(1-t)}$ for B defined as in Assumption D.

Theorem 9. [Theorem 1, Shorack and Wellner (2009)] Suppose Assumptions D and E hold with $\alpha = \max\{b_1 + d_1, b_2 + d_2\} < 1/2$. Then,

$$\sqrt{n}(T_n - \theta) = - \int_0^1 w(1-t)\mathbb{U}_n(t) dh(F_S^{-1}(t)) + o_P(1).$$

Assumption D(a) follows directly from Assumption A. From Assumption B, we know that $\bar{\tau}(q)$ is of bounded variation, and that $\mathbb{E}[|\bar{\tau}(Q)|^r] < \infty$, which implies that we can write

$\bar{\tau}(q) = \bar{\tau}_+(q) - \bar{\tau}_-(q)$, with $\mathbb{E}[|\bar{\tau}_\pm(Q)|^r] < \infty$. Now, Markov's inequality implies that for $s > 0$,

$$P(|\bar{\tau}_\pm(Q)| \geq s) \leq \frac{\mathbb{E}[|\bar{\tau}_\pm(Q)|^r]}{s^r}.$$

Inverting this statement, using the fact that $q \mapsto \bar{\tau}_\pm(q)$ is monotone, we see that Assumption D(b) holds with $d_1 = d_2 = 1/r$. As stipulated in Assumption B, $\alpha = 1/r + b < 1/2$. Therefore, T_n satisfies the assumptions of Theorem 9, implying that it is asymptotically linear with influence function

$$Y_i = \int_{Q_i}^{\infty} w(1 - F(q)) d\bar{\tau}(q) - \theta.$$

The rest of the proof involves showing the remaining terms are asymptotically negligible.

Term 3

For any fixed $\epsilon > 0$, applying Markov's inequality followed by Hölder's inequality gives

$$\begin{aligned} & P \left(\left| \frac{1}{\sqrt{n}} \sum_{i=1}^n \left(w_n(\hat{G}_S(Q_i)) - w(\hat{G}_S(Q_i)) \right) \bar{\tau}(Q_i) \right| \geq \epsilon \right) \\ & \leq \frac{\mathbb{E} \left[\left| \sum_{i=1}^n \left(w_n(\hat{G}_S(Q_i)) - w(\hat{G}_S(Q_i)) \right) \frac{\bar{\tau}(Q_i)}{\sqrt{n}} \right| \right]}{\epsilon} \\ & \leq \frac{\mathbb{E} \left[\left(\sum_{i=1}^n \left(w_n(\hat{G}_S(Q_i)) - w(\hat{G}_S(Q_i)) \right)^p \right)^{1/p} \left(\frac{1}{n^{r/2}} \sum_{i=1}^n |\bar{\tau}|^r(Q_i) \right)^{1/r} \right]}{\epsilon} \end{aligned}$$

Assumption A gives that $\left(\sum_{i=1}^n \left(w_n(\hat{G}_S(Q_i)) - w(\hat{G}_S(Q_i)) \right)^p \right) < C$ eventually. Applying Jensen's inequality shows that $\mathbb{E} \left[\left(\frac{1}{n} \sum_{i=1}^n |\bar{\tau}|^r(Q_i) \right)^{1/r} \right] \leq \mathbb{E}[\bar{\tau}^r(Q_i)]^{1/r}$, which is bounded by Assumption B. Therefore, the numerator is $O(n^{1/2-1/r}) = o(1)$.

Term 4

For any fixed $\epsilon > 0$, applying Chebyshev's inequality conditionally on $\{Q_i\}_{i=1}^n$ shows that

the fourth term satisfies

$$\begin{aligned}
& P \left(\left| \frac{1}{\sqrt{n}} \sum_{i=1}^n \left(w_n(\widehat{G}_S(Q_i)) - w(1 - F_S(Q_i)) \right) (\Gamma_i^* - \bar{\tau}(Q_i)) \right| \geq \epsilon \right) \\
&= \mathbb{E} \left[P \left(\left| \frac{1}{\sqrt{n}} \sum_{i=1}^n \left(w_n(\widehat{G}_S(Q_i)) - w(1 - F_S(Q_i)) \right) (\Gamma_i^* - \bar{\tau}(Q_i)) \right| \geq \epsilon \mid \{Q_i\}_{i=1}^n \right) \right] \\
&= \mathbb{E} \left[\frac{1}{\epsilon^2} \text{Var} \left(\frac{1}{\sqrt{n}} \sum_{i=1}^n \left(w_n(\widehat{G}_S(Q_i)) - w(1 - F_S(Q_i)) \right) (\Gamma_i^* - \bar{\tau}(Q_i)) \mid \{Q_i\}_{i=1}^n \right) \right] \quad (29) \\
&= \frac{1}{\epsilon^2} \mathbb{E} \left[\frac{1}{n} \sum_{i=1}^n \left(w_n(\widehat{G}_S(Q_i)) - w(1 - F_S(Q_i)) \right)^2 \text{Var}(\Gamma_i^* \mid Q_i) \right] \quad (30) \\
&\leq \frac{C_g}{\epsilon^2} \mathbb{E} \left[\frac{1}{n} \sum_{i=1}^n \left(w_n(\widehat{G}_S(Q_i)) - w(1 - F_S(Q_i)) \right)^2 \right],
\end{aligned}$$

where (29) to (30) follows from the rule that $\text{Var}(aX + bY) = a^2\text{Var}(X) + b^2\text{Var}(Y)$, when X and Y are independent, and noting that each term in the sum is independent given $\{Q_i\}_{i=1}^n$. By assumption, $\mathbb{E}[\frac{1}{n} \sum_{i=1}^n (w_n(\widehat{G}_S(Q_i)) - w(1 - F_S(Q_i)))^2] \rightarrow 0$. The last inequality follows from Assumption B.

Term 5

Finally, we control the last term using Assumption C. We begin by splitting the sum up into the K partitions,

$$\frac{1}{\sqrt{n}} \sum_{i=1}^n w_n(\widehat{G}_S(Q_i)) \delta_i = \sum_{k=1}^K \frac{1}{\sqrt{n}} \sum_{i \in I_k} w_n(\widehat{G}_S(Q_i)) \delta_i,$$

and note that because these partitions are selected uniformly at random, it suffices to show that

$$P \left(\left| \frac{1}{\sqrt{n}} \sum_{i \in I_1} w_n(\widehat{G}_S(Q_i)) \delta_i \right| \geq \epsilon \right) \rightarrow 0$$

for any $\epsilon > 0$. Recalling G_1 from Assumption C, we divide this event into a piece that happens on G_1 and a piece that happens on G_1^C ,

$$P \left(\left| \frac{1}{\sqrt{n}} \sum_{i \in I_1} w_n(\widehat{G}_S(Q_i)) \delta_i \right| \geq \epsilon \right) \leq P \left(\left| \frac{1}{\sqrt{n}} \sum_{i \in I_1} w_n(\widehat{G}_S(Q_i)) \delta_i \right| \geq \epsilon \mid G_1 \right) P(G_1) + P(G_1^C).$$

Because $P(G_1) \rightarrow 1$, we need to show that

$$P \left(\left| \frac{1}{\sqrt{n}} \sum_{i \in I_1} w_n(\widehat{G}_S(Q_i)) \delta_i \right| \geq \epsilon \mid G_1 \right) \rightarrow 0.$$

Denote $\{Q_i\}_{i \in I_1}, \{(W_i, X_i, Y_i)\}_{i \notin I_1}$ as B_1 . Using $\xrightarrow{a.s.}$ here to denote convergence almost everywhere on G_1 , it suffices to show that

$$P \left(\left| \frac{1}{\sqrt{n}} \sum_{i \in I_1} w_n(\hat{G}_S(Q_i)) \delta_i \right| \geq \epsilon \mid B_1, G_1 \right) \xrightarrow{a.s.} 0,$$

because the bounded convergence theorem implies that conditional convergence implies unconditional convergence.

If we replace $w_n(\hat{G}_S(Q_i))$ with $w(1 - F_S(Q_i))$ this would follow easily by Chebyshev's inequality from the bias and variance conditions of Assumption C:

$$|\mathbb{E} \left[\frac{1}{\sqrt{n}} \sum_{i \in I_1}^n w(1 - F_S(Q_i)) \delta_i \mid G_1, B_1 \right]| \leq |\sqrt{n} \mathbb{E}[w(1 - F_S(Q_i)) \delta_i \mid B_1, G_1]| \rightarrow 0,$$

and, because we assumed in Assumption C that $\{\delta_i\}_{i \in I_1}$ are independent conditionally on B_1, G_1 ,

$$\text{Var} \left(\frac{1}{\sqrt{n}} \sum_{i \in I_1}^n w(1 - F_S(Q_i)) \delta_i \mid G_1, B_1 \right) = \frac{1}{n} \sum_{i \in I_1} \text{Var} (w(1 - F_S(Q_i)) \delta_i \mid G_1, B_1) \rightarrow 0.$$

This, along with the following lemma proves that Term 5 converges to zero.

Lemma 10. *Under Assumptions A and C,*

$$P \left(\left| \frac{1}{\sqrt{n}} \sum_{i \in I_1} (w_n(\hat{G}_S(Q_i)) - w(1 - F_S(Q_i))) \delta_i \right| \geq \epsilon \mid B_1, G_1 \right) \xrightarrow{a.s.} 0. \quad (31)$$

Proving Lemma 10 is similar to how we control Terms 2-4 in the above decomposition, however now with an L -statistic whose variance goes to 0. See Section A.2.5 in the Supplementary Materials for the details. \square

References

Per Kragh Andersen and Richard D Gill. Cox's regression model for counting processes: a large sample study. *The annals of statistics*, pages 1100–1120, 1982.

Luis M Artigao-Rodenas, Julio A Carbayo-Herencia, Juan A Divison-Garrote, Vicente F Gil-Guillen, Javier Massó-Orozco, Marta Simarro-Rueda, Francisca Molina-Escribano, Carlos Sanchis, Lucinio Carrión-Valero, Enrique Lopez de Coca, et al. Framingham risk score for prediction of cardiovascular diseases: a population-based study from southern Europe. *PLoS one*, 8(9):e73529, 2013.

Eva Ascarza. Retention futility: Targeting high-risk customers might be ineffective. *Journal of Marketing Research*, 55(1):80–98, 2018.

Susan Athey and Guido W Imbens. Machine learning methods that economists should know about. *Annual Review of Economics*, 11:685–725, 2019.

Susan Athey and Stefan Wager. Policy learning with observational data. *Econometrica*, 89(1):133–161, 2021.

Susan Athey, Julie Tibshirani, and Stefan Wager. Generalized random forests. *Annals of Statistics*, 47(2):1148–1178, 2019.

Sanjay Basu, Jeremy B Sussman, and Rod A Hayward. Detecting heterogeneous treatment effects to guide personalized blood pressure treatment: a modeling study of randomized clinical trials. *Annals of internal medicine*, 166(5):354–360, 2017.

Srinivasan Beddhu, Glenn M Chertow, Tom Greene, Paul K Whelton, Walter T Ambrosius, Alfred K Cheung, Jeffrey Cutler, Lawrence Fine, Robert Boucher, Guo Wei, et al. Effects of intensive systolic blood pressure lowering on cardiovascular events and mortality in patients with type 2 diabetes mellitus on standard glycemic control and in those without diabetes mellitus: reconciling results from ACCORD BP and SPRINT. *Journal of the American Heart Association*, 7(18):e009326, 2018.

M Bozorgmanesh, F Hadaegh, and F Azizi. Predictive accuracy of the ‘Framingham’s general CVD algorithm’ in a Middle Eastern population: Tehran Lipid and Glucose Study. *International journal of clinical practice*, 65(3):264–273, 2011.

Leo Breiman. Random forests. *Machine learning*, 45(1):5–32, 2001.

Suzanne J Carroll, Catherine Paquet, Natasha J Howard, Robert J Adams, Anne W Taylor, and Mark Daniel. Validation of continuous clinical indices of cardiometabolic risk in a cohort of Australian adults. *BMC cardiovascular disorders*, 14(1):1–9, 2014.

Victor Chernozhukov, Juan Carlos Escanciano, Hidehiko Ichimura, Whitney K Newey, and James M Robins. Locally robust semiparametric estimation. *arXiv preprint arXiv:1608.00033*, 2016.

Victor Chernozhukov, Denis Chetverikov, Mert Demirer, Esther Duflo, Christian Hansen, Whitney Newey, and James Robins. Double/debiased machine learning for treatment and structural parameters. *The Econometrics Journal*, 21(1):C1–C68, 2018a.

Victor Chernozhukov, Mert Demirer, Esther Duflo, and Ivan Fernandez-Val. Generic machine learning inference on heterogenous treatment effects in randomized experiments. Technical Report, National Bureau of Economic Research, 2018b.

Nancy R Cook, Nina P Paynter, Charles B Eaton, JoAnn E Manson, Lisa W Martin, Jennifer G Robinson, Jacques E Rossouw, Sylvia Wassertheil-Smoller, and Paul M Ridker. Comparison of the Framingham and Reynolds Risk scores for global cardiovascular risk prediction in the multiethnic Women’s Health Initiative. *Circulation*, 125(14):1748–1756, 2012.

Yifan Cui, Michael R Kosorok, Erik Sverdrup, Stefan Wager, and Ruqiang Zhu. Estimating heterogeneous treatment effects with right-censored data via causal survival forests. *arXiv preprint arXiv:2001.09887*, 2020.

Ralph B D'Agostino Sr, Michael J Pencina, Joseph M Massaro, and Sean Coady. Cardiovascular disease risk assessment: insights from Framingham. *Global heart*, 8(1):11–23, 2013.

Andrew P DeFilippis, Rebekah Young, Christopher J Carrubba, John W McEvoy, Matthew J Budoff, Roger S Blumenthal, Richard A Kronmal, Robyn L McClelland, Khurram Nasir, and Michael J Blaha. An analysis of calibration and discrimination among multiple cardiovascular risk scores in a modern multiethnic cohort. *Annals of internal medicine*, 162(4):266–275, 2015.

Eustache Diemert, Artem Betlei, Christophe Renaudin, and Massih-Reza Amini. A Large Scale Benchmark for Uplift Modeling. In *KDD*, 2018.

Peng Ding, Avi Feller, and Luke Miratrix. Randomization inference for treatment effect variation. *Journal of the Royal Statistical Society: Series B: Statistical Methodology*, pages 655–671, 2016.

Tony Duan, Pranav Rajpurkar, Dillon Laird, Andrew Y Ng, and Sanjay Basu. Clinical value of predicting individual treatment effects for intensive blood pressure therapy: A machine learning experiment to estimate treatment effects from randomized trial data. *Circulation: Cardiovascular Quality and Outcomes*, 12(3):e005010, 2019.

A. Dvoretzky, J. Kiefer, and J. Wolfowitz. Asymptotic Minimax Character of the Sample Distribution Function and of the Classical Multinomial Estimator. *The Annals of Mathematical Statistics*, 27(3):642 – 669, 1956. doi: 10.1214/aoms/1177728174. URL <https://doi.org/10.1214/aoms/1177728174>.

Ralph B. D'Agostino, Ramachandran S. Vasan, Michael J. Pencina, Philip A. Wolf, Mark Cobain, Joseph M. Massaro, and William B. Kannel. General Cardiovascular Risk Profile for Use in Primary Care. *Circulation*, 117(6):743–753, 2008. doi: 10.1161/CIRCULATIONAHA.107.699579. URL <https://www.ahajournals.org/doi/abs/10.1161/CIRCULATIONAHA.107.699579>.

Bradley Efron. *The jackknife, the bootstrap and other resampling plans*. SIAM, 1982.

Audes DM Feitosa, Marco A Mota-Gomes, Roberto D Miranda, Weimar S Barroso, Eduardo CD Barbosa, Rodrigo P Pedrosa, Paula C Oliveira, Camila LDM Feitosa, Jose L Lima-Filho, Andrei C Sposito, et al. Impact of 2017 ACC/AHA hypertension guidelines on the prevalence of white-coat and masked hypertension: A home blood pressure monitoring study. *Journal of clinical hypertension (Greenwich, Conn.)*, 20(12):1745–1747, 2018.

Naomi DL Fisher and Gregory Curfman. Hypertension—a public health challenge of global proportions. *Jama*, 320(17):1757–1759, 2018.

Jerome H Friedman. Multivariate adaptive regression splines. *The annals of statistics*, pages 1–67, 1991.

Emmanuela Gakidou, Ashkan Afshin, Amanuel Alemu Abajobir, Kalkidan Hassen Abate, Cristiana Abbafati, Kaja M Abbas, Foad Abd-Allah, Abdishakur M Abdulle, Semaw Ferede Abera, Victor Aboyans, et al. Global, regional, and national comparative risk assessment of 84 behavioural, environmental and occupational, and metabolic risks or clusters of risks, 1990–2016: a systematic analysis for the Global Burden of Disease Study 2016. *The Lancet*, 390(10100):1345–1422, 2017.

David C. Goff, Donald M. Lloyd-Jones, Glen Bennett, Sean Coady, Ralph B. D'Agostino, Raymond Gibbons, Philip Greenland, Daniel T. Lackland, Daniel Levy, Christopher J. O'Donnell, Jennifer G. Robinson, J. Sanford Schwartz, Susan T. Sher, Sidney C. Smith, Paul Sorlie, Neil J. Stone, and Peter W. F. Wilson. 2013 ACC/AHA Guideline on the Assessment of Cardiovascular Risk. *Circulation*, 129(25_suppl_2):S49–S73, 2014. doi: 10.1161/01.cir.0000437741.48606.98. URL <https://www.ahajournals.org/doi/abs/10.1161/01.cir.0000437741.48606.98>.

Brett R Gordon, Florian Zettelmeyer, Neha Bhargava, and Dan Chapsky. A comparison of approaches to advertising measurement: Evidence from big field experiments at Facebook. *Marketing Science*, 38(2):193–225, 2019.

David Marvin Green, John A Swets, et al. *Signal detection theory and psychophysics*, volume 1. Wiley New York, 1966.

ACCORD Study Group. Effects of intensive blood-pressure control in type 2 diabetes mellitus. *New England Journal of Medicine*, 362(17):1575–1585, 2010.

SPRINT Research Group. A randomized trial of intensive versus standard blood-pressure control. *New England Journal of Medicine*, 373(22):2103–2116, 2015.

Trevor Hastie, Robert Tibshirani, and Jerome Friedman. *The elements of statistical learning: data mining, inference, and prediction*. Springer Science & Business Media, 2009.

Jennifer L Hill. Bayesian nonparametric modeling for causal inference. *Journal of Computational and Graphical Statistics*, 20(1):217–240, 2011.

Henning Hohnhold, Deirdre O'Brien, and Diane Tang. Focus on the Long-Term: It's better for Users and Business. In *Proceedings 21st Conference on Knowledge Discovery and Data Mining*, Sydney, Australia, 2015. URL <http://dl.acm.org/citation.cfm?doid=2783258.2788583>.

Chenxi Huang, Sanket S Dhruva, Andreas C Coppi, Frederick Warner, Shu-Xia Li, Haiqun Lin, Khurram Nasir, and Harlan M Krumholz. Systolic blood pressure response in SPRINT (Systolic Blood Pressure Intervention Trial) and ACCORD (Action to Control Cardiovascular Risk in Diabetes): a possible explanation for discordant trial results. *Journal of the American Heart Association*, 6(11):e007509, 2017.

Kosuke Imai and Michael Lingzhi Li. Experimental evaluation of individualized treatment rules. *arXiv preprint arXiv:1905.05389*, 2019.

Guido W Imbens and Donald B Rubin. *Causal inference in statistics, social, and biomedical sciences*. Cambridge University Press, 2015.

Hemant Ishwaran, Udaya B Kogalur, Eugene H Blackstone, Michael S Lauer, et al. Random survival forests. *Annals of Applied Statistics*, 2(3):841–860, 2008.

Garrett A Johnson, Randall A Lewis, and Elmar I Nubbemeyer. Ghost Ads: Improving the Economics of Measuring Online Ad Effectiveness. *Journal of Marketing Research*, 54(6):867–884, 2017.

Daniel W Jones, Paul K Whelton, Norrina Allen, Donald Clark III, Samuel S Gidding, Paul Muntner, Shawna Nesbitt, Nia S Mitchell, Raymond Townsend, Bonita Falkner, et al. Management of Stage 1 Hypertension in Adults With a Low 10-Year Risk for Cardiovascular Disease: Filling a Guidance Gap: A Scientific Statement From the American Heart Association. *Hypertension*, 77(6):e58–e67, 2021.

Sanjay Kaul. A tale of two trials: reconciling differences in results by exploring heterogeneous treatment effects. *Annals of internal medicine*, 166(5):370–372, 2017.

Edward H Kennedy. Optimal doubly robust estimation of heterogeneous causal effects. *arXiv preprint arXiv:2004.14497*, 2020.

David M. Kent, David van Klaveren, Jessica K. Paulus, Ralph D’Agostino, Steve Goodman, Rodney Hayward, John P.A. Ioannidis, Bray Patrick-Lake, Sally Morton, Michael Pencina, Gowri Raman, Joseph S. Ross, Harry P. Selker, Ravi Varadhan, Andrew Vickers, John B. Wong, and Ewout W. Steyerberg. The Predictive Approaches to Treatment effect Heterogeneity (PATH) Statement. *Annals of Internal Medicine*, 172(1):35–45, 2020. doi: 10.7326/M18-3667. URL <https://www.acpjournals.org/doi/abs/10.7326/M18-3667>.

Rohan Khera, Yuan Lu, Jiapeng Lu, Anshul Saxena, Khurram Nasir, Lixin Jiang, and Harlan M Krumholz. Impact of 2017 ACC/AHA guidelines on prevalence of hypertension and eligibility for antihypertensive treatment in United States and China: nationally representative cross sectional study. *Bmj*, 362, 2018.

Leslie Kish and Martin R Frankel. Balanced repeated replications for standard errors. *Journal of the American Statistical Association*, 65(331):1071–1094, 1970.

Sören R Künzel, Jasjeet S Sekhon, Peter J Bickel, and Bin Yu. Metalearners for estimating heterogeneous treatment effects using machine learning. *Proceedings of the national academy of sciences*, 116(10):4156–4165, 2019.

Stephen S Lim, Theo Vos, Abraham D Flaxman, Goodarz Danaei, Kenji Shibuya, Heather Adair-Rohani, Mohammad A AlMazroa, Markus Amann, H Ross Anderson, Kathryn G Andrews, et al. A comparative risk assessment of burden of disease and injury attributable to 67 risk factors and risk factor clusters in 21 regions, 1990–2010: a systematic analysis for the Global Burden of Disease Study 2010. *The lancet*, 380(9859):2224–2260, 2012.

Enno Mammen. *When does bootstrap work?: asymptotic results and simulations*, volume 77. Springer Science & Business Media, 2012.

Charles F Manski. Statistical treatment rules for heterogeneous populations. *Econometrica*, 72(4):1221–1246, 2004.

Paul Muntner, Robert M Carey, Samuel Gidding, Daniel W Jones, Sandra J Taler, Jackson T Wright Jr, and Paul K Whelton. Potential US population impact of the 2017 ACC/AHA high blood pressure guideline. *Circulation*, 137(2):109–118, 2018.

Xinkun Nie and Stefan Wager. Quasi-oracle estimation of heterogeneous treatment effects. *arXiv preprint arXiv:1712.04912*, 2017.

Marco Pahor, Bruce M Psaty, Michael H Alderman, William B Applegate, Jeff D Williamson, Chiara Cavazzini, and Curt D Furberg. Health outcomes associated with calcium antagonists compared with other first-line antihypertensive therapies: a meta-analysis of randomised controlled trials. *The Lancet*, 356(9246):1949–1954, 2000.

Bruce M Psaty, Nicholas L Smith, David S Siscovick, Thomas D Koepsell, Noel S Weiss, Susan R Heckbert, Rozenn N Lemaitre, Edward H Wagner, and Curt D Furberg. Health outcomes associated with antihypertensive therapies used as first-line agents: a systematic review and meta-analysis. *Jama*, 277(9):739–745, 1997.

Bruce M Psaty, Thomas Lumley, Curt D Furberg, Gina Schellenbaum, Marco Pahor, Michael H Alderman, and Noel S Weiss. Health outcomes associated with various antihypertensive therapies used as first-line agents: a network meta-analysis. *Jama*, 289(19):2534–2544, 2003.

Arman Qamar and Eugene Braunwald. Treatment of hypertension: addressing a global health problem. *Jama*, 320(17):1751–1752, 2018.

Amir Qaseem, Timothy J Wilt, Robert Rich, Linda L Humphrey, Jennifer Frost, and Mary Ann Forciea. Pharmacologic treatment of hypertension in adults aged 60 years or older to higher versus lower blood pressure targets: a clinical practice guideline from the American College of Physicians and the American Academy of Family Physicians. *Annals of internal medicine*, 166(6):430–437, 2017.

Nicholas Radcliffe and Patrick Surry. Differential response analysis: Modeling true responses by isolating the effect of a single action. *Credit Scoring and Credit Control IV*, 1999.

Nicholas J Radcliffe. Using control groups to target on predicted lift: Building and assessing uplift models. *Direct Marketing Analytics Journal*, 1(3):14–21, 2007.

Alexandros Rekkas, Jessica K Paulus, Gowri Raman, John B Wong, Ewout W Steyerberg, Peter R Rijnbeek, David M Kent, and David van Klaveren. Predictive approaches to heterogeneous treatment effects: a scoping review. *BMC Medical Research Methodology*, 20(1):1–12, 2020.

James M Robins, Andrea Rotnitzky, and Lue Ping Zhao. Estimation of regression coefficients when some regressors are not always observed. *Journal of the American statistical Association*, 89(427):846–866, 1994.

Paul R Rosenbaum and Donald B Rubin. The central role of the propensity score in observational studies for causal effects. *Biometrika*, 70(1):41–55, 1983.

Vira Semenova and Victor Chernozhukov. Debiased machine learning of conditional average treatment effects and other causal functions. *arXiv preprint arXiv:1702.06240*, 2017.

Galen R Shorack. Functions of order statistics. *The Annals of Mathematical Statistics*, 43(2):412–427, 1972.

Galen R Shorack and Jon A Wellner. *Empirical Processes with Applications to Statistics*. SIAM, 2009.

George CM Siontis, Ioanna Tzoulaki, Konstantinos C Siontis, and John PA Ioannidis. Comparisons of established risk prediction models for cardiovascular disease: systematic review. *Bmj*, 344, 2012.

Hao Sun, Shuyang Du, and Stefan Wager. Treatment Allocation under Uncertain Costs. *arXiv preprint arXiv:2103.11066*, 2021.

Terry M Therneau and Patricia M Grambsch. The cox model. In *Modeling survival data: extending the Cox model*, pages 39–77. Springer, 2000.

Anastasios Tsiatis. *Semiparametric theory and missing data*. Springer Science & Business Media, 2007.

Thomas Unger, Claudio Borghi, Fadi Charchar, Nadia A. Khan, Neil R. Poulter, Dorrairaj Prabhakaran, Agustin Ramirez, Markus Schlaich, George S. Stergiou, Maciej Tomaszewski, Richard D. Wainford, Bryan Williams, and Aletta E. Schutte. 2020 International Society of Hypertension Global Hypertension Practice Guidelines. *Hypertension*, 75(6):1334–1357, 2020. doi: 10.1161/HYPERTENSIONAHA.120.15026. URL <https://www.ahajournals.org/doi/abs/10.1161/HYPERTENSIONAHA.120.15026>.

Aad W Van Der Vaart and Jon A Wellner. Weak convergence. In *Weak convergence and empirical processes*, pages 16–28. Springer, 1996.

Stefan Wager and Susan Athey. Estimation and inference of heterogeneous treatment effects using random forests. *Journal of the American Statistical Association*, 113(523):1228–1242, 2018.

Paul K Whelton, Robert M Carey, Wilbert S Aronow, Donald E Casey, Karen J Collins, Cheryl Dennison Himmelfarb, Sondra M DePalma, Samuel Gidding, Kenneth A Jamerson, Daniel W Jones, et al. 2017 ACC/AHA/AAPA/ABC/ACPM/AGS/APhA/ASH/ASPC/NMA/PCNA guideline for the prevention, detection, evaluation, and management of high blood pressure in adults: a report of the American College of Cardiology/American Heart Association Task

Force on Clinical Practice Guidelines. *Journal of the American College of Cardiology*, 71 (19):e127–e248, 2018.

Steve Yadlowsky, Rodney A Hayward, Jeremy B Sussman, Robyn L McClelland, Yuan-I Min, and Sanjay Basu. Clinical implications of revised pooled cohort equations for estimating atherosclerotic cardiovascular disease risk. *Annals of internal medicine*, 169 (1):20–29, 2018.

Lihui Zhao, Lu Tian, Tianxi Cai, Brian Claggett, and Lee-Jen Wei. Effectively selecting a target population for a future comparative study. *Journal of the American Statistical Association*, 108(502):527–539, 2013.

Mark H Zweig and Gregory Campbell. Receiver-operating characteristic (ROC) plots: a fundamental evaluation tool in clinical medicine. *Clinical chemistry*, 39(4):561–577, 1993.

Aad W. van der Vaart. *Asymptotic Statistics*. Cambridge Series in Statistical and Probabilistic Mathematics. Cambridge University Press, 1998.

A SUPPLEMENT

A.1 Precise Converse to Proposition 3

Proposition 11. Suppose that $S(X_i)$ has no ties, i.e., that $F_S(X_i)$ has a uniform distribution on $[0, 1]$, and that $\tau(x) = \mathbb{E}[Y_i(1) - Y_i(0) \mid X_i = x]$ is uniformly bounded. Furthermore, suppose that $w : [0, 1] \rightarrow \mathbb{R}$ admits a (Radon-Nikodym) derivative $w'(u)$ such that $w'(u)(1-u)$ is absolutely integrable with respect to Lebesgue measure on $[0, 1]$, and that $\int_0^1 w(u) du = 0$. Then $\eta_w(S)$ as defined in (9) is a RATE in the sense of Definition 3, with the weight function defined in Eq. 10 reproduced here:

$$\eta_w(S) = \theta_{\alpha_w}(S), \quad \alpha_w(t) = -tw'(1-t).$$

Proof We first note that, by the chain rule, $\eta_w = \mathbb{E}[w(1 - F_S(S(X_i))) \tau(X_i)]$, and furthermore

$$\begin{aligned} \eta_w(S) &= \int w(1 - F_S(S(x))) \tau(x) d\mathbb{P}(x) \\ &= w(1)\mathbb{E}[\tau(X)] - \int \int_0^{F_S(S(x))} w'(1-u) du \tau(x) d\mathbb{P}(x) \\ &= w(1)\mathbb{E}[\tau(X)] - \int \int_0^1 1(\{u \leq F_S(S(x))\}) w'(1-u) du \tau(x) d\mathbb{P}(x). \end{aligned}$$

Next, because $(1-u)w'(u)$ is absolutely integrable and $\tau(x)$ (and thus also the TOC) is

uniformly bounded, we can use Fubini's theorem to continue, and verify that

$$\begin{aligned}
\eta_w(S) &= w(1)\mathbb{E}[\tau(X)] - \int_0^1 w'(1-u) \int 1\left(\{u \leq F_S(S(x))\}\right) \tau(x) d\mathbb{P}(x) du \\
&= w(1)\mathbb{E}[\tau(X)] - \int_0^1 w'(1-u) (1-u) \left(\text{TOC}(u; S) + \mathbb{E}[\tau(X)]\right) du \\
&= \theta_{\alpha_w}(S) + \mathbb{E}[\tau(X)] \left(w(1) - \int_0^1 w'(1-u) (1-u) du\right),
\end{aligned}$$

where $\theta_{\alpha_w}(S)$ is as defined in (3). Finally, integrating by parts, we see that $\int_0^1 w'(1-u) (1-u) du = \int_0^1 w'(u)u du = w(1) - \int_0^1 w(u) du = w(1)$ because $\int_0^1 w(u) du = 0$ by assumption, and so $\eta_w(S) = \theta_{\alpha_w}(S)$. \square

A.2 Proofs

A.2.1 Proof of Corollary 5

Proof Throughout, we will assume that n is divisible by two for notational simplicity.

The key is the following lemma, with which, the Corollary follows directly from Theorem 4.

Lemma 12. *For some parameter β , let $\hat{\beta}$ be an estimator from iid data $(Z_i)_{i=1}^n$ that satisfies $\sqrt{n}(\hat{\beta} - \beta) = \frac{1}{\sqrt{n}} \sum_{i=1}^n \psi(Z_i) + o_P(1) \xrightarrow{d} Z$ for a fixed, measurable function ψ such that $\mathbb{E}[\psi^2(Z_i)] < \infty$ and $\mathbb{E}[\psi(Z_i)] = 0$. Let $\hat{\beta}^*$ be the estimate using a random sample (without replacement) of $n/2$ of the Z_i . Then, conditionally on $(Z_i)_{i=1}^n$, $\sqrt{n}(\hat{\beta}^* - \hat{\beta}) \xrightarrow{d} Z$, as well.*

Proof of Lemma Because $\sqrt{n}(\hat{\beta} - \beta) = \frac{1}{\sqrt{n}} \sum_{i=1}^n \psi(Z_i) + o_P(1)$, when fit with $n/2$ samples, we have that $\sqrt{n}(\hat{\beta}^* - \beta) = \sqrt{n} \frac{2}{n} \sum_{i=1}^{n/2} \psi(Z_i) + o_P(1)$.

Write $\sqrt{n}(\hat{\beta}^* - \hat{\beta})$ as the difference between the two terms above,

$$\begin{aligned}
\sqrt{n}(\hat{\beta}^* - \hat{\beta}) &= \sqrt{n}(\hat{\beta}^* - \beta) - \sqrt{n}(\hat{\beta} - \beta) \\
&= \frac{1}{\sqrt{n}} \sum_{i=1}^{n/2} V_i \psi(Z_i) + o_P(1),
\end{aligned} \tag{32}$$

where V_i is 1 if the i -th example is in the subset of $n/2$ examples in the bootstrap sample, and otherwise is -1 .

Our goal is to show that this is (conditionally) asymptotically normal with distribution $\mathbb{N}(0, \text{Var}(\psi(Z_i)))$. Because $\sqrt{n}(\hat{\beta} - \beta) \xrightarrow{d} Z$, with $Z \sim \mathbb{N}(0, \text{Var}(\psi(Z_i)))$, this will prove the result.

To show that this is true, we first consider a “binomialized” version of the term (32).⁶ Let N_n be a random draw from a $\text{Ber}(n, \frac{1}{2})$ distribution. If $N_n > n/2$, randomly choose $N_n - n/2$

⁶This technique is inspired by the Poissonization proof technique for the standard empirical bootstrap as in (Van Der Vaart and Wellner, 1996, Chp. 3.6).

samples with $V_i = -1$ and set $\tilde{V}_i = 1$. If $N_n < n/2$, randomly choose $n/2 - N_n$ samples with $V_i = 1$ and set $\tilde{V}_i = -1$. Set $\tilde{V}_i = V_i$ for all other samples. With this construction, $\{\tilde{V}_i\}_{i=1}^n$ are i.i.d. Rademacher random variables,

$$\tilde{V}_i = \begin{cases} 1 & \text{w.p. } \frac{1}{2} \\ -1 & \text{w.p. } \frac{1}{2}. \end{cases}$$

Therefore, the multiplier central limit theorem (Van Der Vaart and Wellner, 1996, Lemma 2.9.5) implies that

$$\frac{1}{\sqrt{n}} \sum_{i=1}^n \tilde{V}_i \psi(Z_i)$$

converges to $\mathsf{N}(0, \text{Var}(\psi(Z_i)))$, conditionally on $(Z_i)_{i=1}^n$ almost surely.

To complete the proof, we need to show that conditionally (almost surely) on $(Z_i)_{i=1}^n$,

$$R_n(N_n) = \frac{1}{\sqrt{n}} \sum_{i=1}^n (\tilde{V}_i - V_i) \psi(Z_i) = o_P(1).$$

Towards this goal, first notice that $V_i - \tilde{V}_i$ is only nonzero on the $|N_n - n/2|$ samples changed in the construction of \tilde{V}_i . Let I_n be the indices of these samples. Then, observe that

$$R_n(N_n) = \text{sign}(N_n - n/2) \frac{2}{\sqrt{n}} \sum_{i \in I_n} \psi(Z_i).$$

Inspecting the symmetry of $R_n(N_n)$, we can see that because N_n is symmetric about $n/2$, $\tilde{\mathbb{E}}[R_n(N_n)] = 0$, with $\tilde{\mathbb{E}}[\cdot]$ shorthand for $\mathbb{E}[\cdot \mid \{Z_i\}_{i=1}^n]$. Our approach, then, is to show that $\widetilde{\text{Var}}(R_n(N_n)) \xrightarrow{a.s.} 0$, where $\widetilde{\text{Var}}(\cdot) = \text{Var}(\cdot \mid \{Z_i\}_{i=1}^n)$ which by Chebyshev's inequality, implies $P(|R_n(N_n)| > \epsilon \mid \{Z_i\}_{i=1}^n) \rightarrow 0$, as claimed.

To bound the variance, we start by applying the law of total variance,

$$\widetilde{\text{Var}}(R_n(N_n)) = \widetilde{\text{Var}}\left(\tilde{\mathbb{E}}\left[R_n(N_n) \mid N_n\right]\right) + \tilde{\mathbb{E}}\left[\widetilde{\text{Var}}(R_n(N_n) \mid N_n)\right],$$

and note that conditional on N_n , the remaining randomness is the choice of $|N_n - n/2|$ samples in I_n . In this way,

$$\sum_{i \in I_n} \psi(Z_i)$$

is naturally interpretable as $A_n := |N_n - n/2|$ times the sample average of A_n randomly drawn points $\psi(Z_i)$ from the finite population $\{\psi(Z_i)\}_{i=1}^n$. With this in mind,

$$\begin{aligned} \tilde{\mathbb{E}}\left[\sum_{i \in I_n} \psi(Z_i) \mid N_n\right] &= \frac{A_n}{n} \sum_{i=1}^n \psi(Z_i) \\ \widetilde{\text{Var}}\left(\sum_{i \in I_n} \psi(Z_i) \mid N_n\right) &= A_n \frac{n - A_n}{n} \left(\frac{1}{n-1} \sum_{i=1}^n \psi^2(Z_i) - \left(\frac{1}{n-1} \sum_{i=1}^n \psi(Z_i) \right)^2 \right). \end{aligned}$$

Plugging these expressions into $R_n(N_n)$ gives

$$\widetilde{\mathbb{E}} \left[R_n(N_n) \mid N_n \right] = \frac{2}{\sqrt{n}} \frac{N_n - n/2}{n} \sum_{i=1}^n \psi(Z_i)$$

and so

$$\widetilde{\text{Var}} \left(\widetilde{\mathbb{E}} \left[R_n(N_n) \mid N_n \right] \right) = \frac{4}{n} \widetilde{\text{Var}}(N_n) \left(\frac{1}{n} \sum_{i=1}^n \psi(Z_i) \right)^2 = \left(\frac{1}{n} \sum_{i=1}^n \psi(Z_i) \right)^2 \quad (33)$$

and

$$\widetilde{\mathbb{E}} \left[\widetilde{\text{Var}} \left(R_n(N_n) \mid N_n \right) \right] = \widetilde{\mathbb{E}} \left[\frac{4A_n(n - A_n)}{n^2} \right] \underbrace{\left(\frac{1}{n-1} \sum_{i=1}^n \psi^2(Z_i) - \left(\frac{1}{n-1} \sum_{i=1}^n \psi(Z_i) \right)^2 \right)}_{s_\psi^2}. \quad (34)$$

Term (33) converges to zero almost surely by the Strong Law of Large Numbers. Term (34) also converges to zero almost surely, because $(n - A_n)/n \leq 1$, $\widetilde{\mathbb{E}} [A_n/n] \asymp 1/\sqrt{n}$, and $s_\psi^2 \rightarrow \text{Var}(\psi(Z_i))$ almost surely by the Strong Law. \square

Theorem 4 shows that $\widehat{\theta}$ satisfies the assumptions of the lemma, completing the proof of the corollary. \square

A.2.2 Proof of Lemma 6

Proof Define $\widehat{G}_S(q)$ as in the proof of Theorem 4 in Section 8, and let $G_S(q)$ be the corresponding distribution function of $S(X_i)$ in reverse order. By continuity, we know that $|w(\widehat{G}_S(S(X_i))) - w(1 - F_S(S(X_i)))| \leq \rho_w(|\widehat{G}_S(S(X_i)) - G_S(S(X_i))|)$, where ρ_w is the modulus of continuity of w . By the monotonicity of ρ_w , $\rho_w(|\widehat{G}_S(S(X_i)) - G_S(S(X_i))|) \leq \rho_w(\|\widehat{G} - G\|_\infty)$. Therefore, $\frac{1}{n} \sum_{i=1}^n (w(\widehat{G}_S(S(X_i))) - w(G_S(S(X_i))))^2 \leq \rho_w^2(\|\widehat{G} - G\|_\infty)$. The Glivenko-Cantelli Theorem shows that $\|\widehat{G} - G\|_\infty \rightarrow 0$ almost surely, and so the claimed statement holds due to the bounded convergence theorem, as \widehat{G} and G are bounded in $[0, 1]$, implying that $\rho_w(\|\widehat{G} - G\|_\infty)$ is bounded, as well. \square

A.2.3 Proof of Proposition 8

Proof Define $\widehat{G}_S(q)$ as in the proof of Theorem 4 in Section 8, and let $G_S(q)$ be the corresponding distribution function of $S(X_i)$ in reverse order. Writing

$$\begin{aligned} & \mathbb{E}\left[\frac{1}{n} \sum_{i=1}^n (w_n(\widehat{G}_S(S(X_i))) - w(G_S(S(X_i))))^2\right] \\ & \leq \underbrace{\frac{2}{n} \sum_{i=1}^n (w_n(i/n) - w(i/n))^2}_{\text{Part 1}} + \underbrace{\mathbb{E}\left[\frac{2}{n} \sum_{i=1}^n (-\log(\widehat{G}_S(Q_i)) + \log(G_S(Q_i)))^2\right]}_{\text{Part 2}}, \end{aligned}$$

we verify that each of these terms vanishes in the following steps:

1. Showing that Part 1 is $O(1)$, then
2. showing that Part 2 vanishes.

Step 1: Recall that $w_n(i/n) = H_n - H_i - 1$ and $w(i/n) = \log(n) - \log(i) - 1$. Noting that $|H_n - H_k - \log(n) + \log(k)| \leq \frac{1}{2k}$ for $1 \leq k \leq n$, averaging over these differences gives

$$\sum_{i=1}^n (w_n(i/n) - w(i/n))^2 \leq \sum_{i=1}^n \frac{1}{(2i)^2} \leq \frac{\pi^2}{24}.$$

This verifies the second part of Assumption A. Additionally, $\frac{1}{n} \sum_{i=1}^n (w_n(i/n) - w(i/n))^2 \rightarrow 0$, showing that the first term of the above decomposition vanishes.

Step 2: In this step, we bound the squared difference between $w \circ \widehat{G}_S$ and $w \circ G_S$ in the following sense:

$$\mathbb{E}\left[\frac{1}{n} \sum_{i=1}^n (-\log(\widehat{G}_S(Q_i)) + \log(G_S(Q_i)))^2\right] = o(1).$$

We make the following observation, with proof in the following section, that shows that it is sufficient to control $(-\log(\widehat{G}_S(Q_i)) + \log(G_S(Q_i)))^2$ on the event $G_S(Q_i) \geq n^{\epsilon-1}/2, \widehat{G}_S(Q_i) \geq n^{\epsilon-1}$.

Lemma 13. For any $1/2 < \epsilon < 1$,

$$\begin{aligned} & \mathbb{E}\left[\frac{1}{n} \sum_{i=1}^n (-\log(\widehat{G}_S(Q_i)) + \log(G_S(Q_i)))^2\right] \\ & = \underbrace{\mathbb{E}\left[\mathbf{1}\left\{\widehat{G}_S(Q_i) \geq n^{\epsilon-1}, G_S(Q_i) \geq n^{\epsilon-1}/2\right\} (-\log(\widehat{G}_S(Q_i)) + \log(G_S(Q_i)))^2\right]}_{(*)} + o(1). \end{aligned}$$

To control the expectation (*), we do a Taylor expansion and apply the DKW inequality. For some $0 < s < 1$,

$$(-\log(\widehat{G}_S(Q_i)) + \log(G_S(Q_i)))^2 \leq \left(-\frac{\widehat{G}_S(Q_i) - G_S(Q_i)}{\widehat{G}_S(Q_i)} - \frac{(\widehat{G}_S(Q_i) - G_S(Q_i))^2}{(s\widehat{G}_S(Q_i) + (1-s)G_S(Q_i))^2} \right)^2.$$

On the event $\{\widehat{G}_S(Q_i) \geq n^{\epsilon-1}, G_S(Q_i) \geq n^{\epsilon-1}/2\}$, this is bounded by

$$\begin{aligned} &\leq n^{2(1-\epsilon)}(\widehat{G}_S(Q_i) - G_S(Q_i))^2 \\ &\quad + 16n^{4(1-\epsilon)}(\widehat{G}_S(Q_i) - G_S(Q_i))^4 \\ &\leq n^{2(1-\epsilon)}\|\widehat{G}_S - G_S\|_\infty^2 + 16n^{4(1-\epsilon)}\|\widehat{G}_S - G_S\|_\infty^4. \end{aligned}$$

Dvoretzky et al. (1956) shows that $P(\|\widehat{G}_S - G_S\|_\infty > t) \leq 2\exp(-Cn t^2)$ for some $0 < C < \infty$. Using that for a random variable $V > 0$ and exponent $r \geq 1$, we have $\mathbb{E}[V^r] \leq \int_0^\infty t^{r-1} P(V > t) dt$, we can bound

$$\begin{aligned} (*) &\leq \mathbb{E}[n^{2(1-\epsilon)}\|\widehat{G}_S - G_S\|_\infty^2 + 16n^{4(1-\epsilon)}\|\widehat{G}_S - G_S\|_\infty^4] \\ &\leq n^{2(1-\epsilon)} \int_0^\infty t \exp(-Cn t^2) dt + 16n^{4(1-\epsilon)} \int_0^\infty t^3 \exp(-Cn t^2) dt \\ &\leq \frac{n^{2(1-\epsilon)}}{2Cn} + \frac{16n^{4(1-\epsilon)}}{2C^2 n^2} = \frac{1}{2C} n^{1-2\epsilon} + \frac{8}{C^2} n^{2-4\epsilon}. \end{aligned}$$

This vanishes as $n \rightarrow \infty$ so long as $\epsilon > 1/2$. \square

A.2.4 Proof of Lemma 13

Proof We continue to use the notation for $\widehat{G}_S(q)$ as in the proof of Theorem 4 in Section 8, and use $G_S(q)$ be the corresponding distribution function of $S(X_i)$ in reverse order. First, we split the term into two parts,

$$\begin{aligned} &\mathbb{E} \left[\frac{1}{n} \sum_{i=1}^n (-\log(\widehat{G}_S(Q_i)) + \log(G_S(Q_i)))^2 \right] \\ &= \underbrace{\mathbb{E} \left[\frac{1}{n} \sum_{j=1}^{n^\epsilon} (-\log(\widehat{G}_S(Q_{i(j)})) + \log(G_S(Q_{i(j)})))^2 \right]}_{=: R_1} + \mathbb{E} \left[\frac{1}{n} \sum_{j=n^\epsilon}^n (-\log(\widehat{G}_S(Q_{i(j)})) + \log(G_S(Q_{i(j)})))^2 \right]. \end{aligned}$$

The first step of the proof is to show that $R_1 = o(1)$, and the second step is to show that additionally conditioning the second term on $G_S(Q_{i(j)}) > n^{\epsilon-1}/2$ has an asymptotically negligible effect on the expectation.

Step 1: Let U_i be iid uniform random variables on $[0, 1]$, and $U_{i(1)}$ be the minimum of U_1, \dots, U_n . The key to this step is a change of variables from Q_i to U_i . Let $f_{U_{i(1)}}(u)$ be its density,

$$f_{U_{i(1)}}(u) = n(1 - u)^{n-1}.$$

By the monotonicity of the order statistics $Q_{i(j)}$, $t \mapsto G_S(t)$ and $t \mapsto \log t$,

$$\begin{aligned} \mathbb{E}[\log^2(G_S(Q_{i(j})))] &\leq \mathbb{E}[\log(G_S(Q_{i(1)}))] \\ &= \int \log^2(u) f_{U_{i(1)}}(u) \, du \\ &= \frac{6nH_n^2 - 6n\psi^{(1)}(n+1) + 6n\pi^2}{6n} \leq H_n^2 + \pi^2. \end{aligned}$$

Along with the fact that at all of the observed samples $\{Q_i\}_{i=1}^n$, used to construct $\widehat{G}_S(\cdot)$, $1/n \leq \widehat{G}_S(Q_i) \leq 1$, this allows us to bound R_1 as

$$\begin{aligned} R_1 &= \mathbb{E} \left[\frac{1}{n} \sum_{j=1}^{n^\epsilon} (-\log(\widehat{G}_S(Q_{i(j)})) + \log(G_S(Q_{i(j)})))^2 \right] \\ &\leq \mathbb{E} \left[\frac{1}{n} \sum_{j=1}^{n^\epsilon} 2\log^2(\widehat{G}_S(Q_{i(j)})) + 2\log^2(G_S(Q_{i(j)})) \right] \\ &\leq \frac{2\log^2(n) + 2H_n^2 + 2\pi^2}{n^{1-\epsilon}} \rightarrow 0 \end{aligned}$$

because $\epsilon < 1$.

Step 2: Notice that the sum $\mathbb{E} \left[\frac{1}{n} \sum_{j=n^\epsilon}^n (-\log(\widehat{G}_S(Q_{i(j)})) + \log(G_S(Q_{i(j)})))^2 \right]$ is over all indices i such that $\widehat{G}_S(Q_i) \geq n^{\epsilon-1}$, therefore we can rewrite the sum as

$$\begin{aligned} &\mathbb{E} \left[\frac{1}{n} \sum_{j=n^\epsilon}^n (-\log(\widehat{G}_S(Q_{i(j)})) + \log(G_S(Q_{i(j)})))^2 \right] \\ &= \mathbb{E} \left[\frac{1}{n} \sum_{i=1}^n \mathbf{1} \left\{ \widehat{G}_S(Q_i) \geq n^{\epsilon-1} \right\} (-\log(\widehat{G}_S(Q_i)) + \log(G_S(Q_i)))^2 \right], \end{aligned}$$

so that each term of the sum is identically distributed. By linearity of expectation, this is equal to

$$\mathbb{E} \left[\mathbf{1} \left\{ \widehat{G}_S(Q_i) \geq n^{\epsilon-1} \right\} (-\log(\widehat{G}_S(Q_i)) + \log(G_S(Q_i)))^2 \right]$$

Splitting this expectation into two events, $\{G_S(Q_i) \geq n^{\epsilon-1}/2\}$ and $\{G_S(Q_i) < n^{\epsilon-1}/2\}$, we

show that the latter event is rare enough to contribute negligibly to the expectation:

$$\begin{aligned}
& \mathbb{E} \left[\mathbf{1} \left\{ \widehat{G}_S(Q_i) \geq n^{\epsilon-1}, G_S(Q_i) < n^{\epsilon-1}/2 \right\} (-\log(\widehat{G}_S(Q_i)) + \log(G_S(Q_i)))^2 \right] \\
& \leq \mathbb{E} \left[2\log^2(n) + 2\log^2(U) \mid U \leq n^{\epsilon-1}/2 \right] P \left(\widehat{G}_S(Q_i) \geq n^{\epsilon-1}, G_S(Q_i) < n^{\epsilon-1}/2 \right) \\
& = O(\log(n) + \log^2(n)) P \left(\widehat{G}_S(Q_i) \geq n^{\epsilon-1}, G_S(Q_i) < n^{\epsilon-1}/2 \right) \\
& \leq O(\log(n) + \log^2(n)) P \left(\|\widehat{G}_S(\cdot) - G_S(\cdot)\|_{\infty} > n^{\epsilon-1}/2 \right)
\end{aligned}$$

Dvoretzky et al. (1956) shows that $P(\|\widehat{G}_S - G_S\|_{\infty} > t) \leq 2 \exp(-Cn t^2)$ for some $0 < C < \infty$, so the above is bounded by

$$O(\log(n) + \log^2(n)) \exp(-Cn^{2\epsilon-1}/4)$$

which converges to 0 as $n \rightarrow \infty$, because $\epsilon > 1/2$. \square

A.2.5 Proof of Lemma 10

Proof Throughout this proof, we will do everything implicitly conditional on B_1 and G_1 . We split the term (31) into three terms,

$$\begin{aligned}
& \frac{1}{\sqrt{n}} \sum_{i \in I_1} (w_n(\widehat{G}_S(Q_i)) - w(1 - F_S(Q_i))) \delta_i \\
& = \underbrace{\frac{1}{\sqrt{n}} \sum_{i \in I_1} (w_n(\widehat{G}_S(Q_i)) - w(1 - F_S(Q_i))) (\delta_i - \mathbb{E}[\delta_i \mid Q_i])}_{\text{Term 1}} \\
& + \underbrace{\frac{1}{\sqrt{n}} \sum_{i \in I_1} (w_n(\widehat{G}_S(Q_i)) - w(\widehat{G}_S(Q_i))) \mathbb{E}[\delta_i \mid Q_i]}_{\text{Term 2}} \\
& + \underbrace{\frac{1}{\sqrt{n}} \sum_{i \in I_1} (w(\widehat{G}_S(Q_i)) - w(1 - F_S(Q_i))) \mathbb{E}[\delta_i \mid Q_i]}_{\text{Term 3}}.
\end{aligned}$$

Under the assumptions of this Lemma, each of these terms converges in probability to zero, as we now show. The first term is mean zero, and therefore, that it is negligible follows from

Chebyshev's inequality and Assumption A

$$\begin{aligned}
& P \left(\left| \frac{1}{\sqrt{n}} \sum_{i \in I_1} (w_n(\widehat{G}_S(Q_i)) - w(1 - F_S(Q_i)))(\delta_i - \mathbb{E}[\delta_i | Q_i]) \right| > \epsilon \right) \\
& \leq \frac{\text{Var} \left(\frac{1}{\sqrt{n}} \sum_{i \in I_1} (w_n(\widehat{G}_S(Q_i)) - w(1 - F_S(Q_i)))(\delta_i - \mathbb{E}[\delta_i | Q_i]) \right)}{\epsilon^2} \\
& = \frac{\mathbb{E} \left[\text{Var} \left(\frac{1}{\sqrt{n}} \sum_{i \in I_1} (w_n(\widehat{G}_S(Q_i)) - w(1 - F_S(Q_i)))(\delta_i - \mathbb{E}[\delta_i | Q_i]) \mid \{Q_i\}_{i=1}^n \right) \right]}{\epsilon^2} \\
& = \frac{\mathbb{E} \left[\frac{1}{n} \sum_{i \in I_1} (w_n(\widehat{G}_S(Q_i)) - w(1 - F_S(Q_i)))^2 \mathbb{E}[\delta_i^2 | Q_i] \right]}{\epsilon^2} \\
& \leq \frac{C}{\epsilon^2} \mathbb{E} \left[\frac{1}{n} \sum_{i \in I_1} (w_n(\widehat{G}_S(Q_i)) - w(1 - F_S(Q_i)))^2 \right] \rightarrow 0.
\end{aligned}$$

Similarly, the second term follows from applying Hölder's inequality to show that the second moment of the second term goes to zero, and applying Markov's inequality,

$$\begin{aligned}
& P \left(\left| \frac{1}{\sqrt{n}} \sum_{i \in I_1} (w_n(\widehat{G}_S(Q_i)) - w(\widehat{G}_S(Q_i))) \mathbb{E}[\delta_i | Q_i] \right| > \epsilon^2 \right) \\
& \leq \frac{\mathbb{E} \left[\left| \frac{1}{\sqrt{n}} \sum_{i \in I_1} (w_n(\widehat{G}_S(Q_i)) - w(\widehat{G}_S(Q_i))) \mathbb{E}[\delta_i | Q_i] \right| \right]}{\epsilon} \\
& \leq \frac{\mathbb{E} \left[\sqrt{\sum_{i \in I_1} (w_n(\widehat{G}_S(Q_i)) - w(\widehat{G}_S(Q_i)))^2 \frac{1}{n} \sum_{i \in I_1} \mathbb{E}[\delta_i | Q_i]^2} \right]}{\epsilon} \\
& = \frac{\sqrt{\sum_{j=1}^n (w_n(j/n) - w(j/n))^2}}{\epsilon} \mathbb{E} \left[\sqrt{\frac{1}{n} \sum_{i \in I_1} \mathbb{E}[\delta_i | Q_i]^2} \right] \\
& \leq \frac{\sqrt{\sum_{j=1}^n (w_n(j/n) - w(j/n))^2}}{\epsilon} \sqrt{\mathbb{E} \left[\frac{1}{n} \sum_{i \in I_1} \mathbb{E}[\delta_i | Q_i]^2 \right]}.
\end{aligned}$$

Assumption A implies

$$\frac{\sum_{j=1}^n (w_n(j/n) - w(j/n))^2}{\epsilon^2}$$

is bounded eventually, and Assumption C implies

$$\mathbb{E} \left[\frac{1}{n} \sum_{i \in I_1} \mathbb{E}[\delta_i | Q_i]^2 \right] \rightarrow 0.$$

Therefore, Term 2 is $o_P(1)$.

The third term is an L -statistic in the sense of [Shorack \(1972\)](#), which differs from [Shorack and Wellner \(2009\)](#) in that it allows the function of the L -statistic to vary with n , which is important when working with the approximation errors δ_i . Specifically, they study estimators of the form

$$T_n = \frac{1}{n} \sum_{j=1}^n c_{nj} g_n(\xi_{nj})$$

where, for our purposes, $c_{ni} = w(j/n)$ and ξ_{nj} is an order statistic of a uniform random variable. Because we have assumed that the distribution function $F_S(\cdot)$ of Q is continuous, we can define $g_n(t) = \mathbb{E}[\delta_i \mid Q_i = F_S^{-1}(t)]$, and $g(t) = 0$. We proceed by showing that Assumptions 1-3 of [Shorack \(1972\)](#) hold (Assumption 4 is not needed, because we have assumed that what [Shorack \(1972\)](#) calls κ is 0). From this, we can conclude that $\sqrt{n}(T_n - \mu_n) \xrightarrow{p} 0$, where $\mu_n = \mathbb{E}[w(1 - F_S(Q_i))\mathbb{E}[\delta_i \mid Q_i]]$. Notice that μ_n is also the mean of

$$T'_n = \frac{1}{n} \sum_{i=1}^n w(1 - F_S(Q_i))\mathbb{E}[\delta_i \mid Q_i],$$

and that each of these terms is independent. Therefore, Chebyshev's inequality implies $\sqrt{n}(T'_n - \mu_n) \xrightarrow{p} 0$, because $|w(1 - F_S(Q_i))\mathbb{E}[\delta_i \mid Q_i]|^2 \leq \mathbb{E}[w^2(1 - F_S(Q_i))\delta_i^2] \rightarrow 0$ from Assumption [C](#). Altogether, this implies that $\sqrt{n}(T_n - T'_n) \xrightarrow{p} 0$, which is exactly Term 3. Therefore, the proof follows from showing that Assumptions 1-3 of [Shorack \(1972\)](#) hold.

In this, to avoid conflicting notation, we shall use ϵ in place of the δ using in [Shorack \(1972\)](#). To satisfy Assumption 1 of [Shorack \(1972\)](#), let $b_1 = b_2 = b$ as defined in Assumption [A](#), so that the conditions on J hold. Using that $\mathbb{E}[|\delta_i|^r] < \infty$ in Assumption [C](#), Markov's inequality gives

$$P(|\mathbb{E}[\delta_i \mid Q_i]| \geq s) \leq \frac{\mathbb{E}[|\mathbb{E}[\delta_i \mid Q_i]|^r]}{s^r} \leq \frac{\mathbb{E}[|\delta_i|^r]}{s^r}.$$

Inverting this statement, using that $\mathbb{E}[\delta_i \mid Q_i]$ is of bounded variation and so can be split into two monotone functions, gives $|g_n(t)| \leq C(t(1-t))^{1/r}$. Since the condition on r and b from Assumption [B](#) implies there exists $\epsilon' > 0$ such that $1/r + b + \epsilon' \leq 1/2$, Assumption 1 of [Shorack \(1972\)](#) holds with ϵ being the minimum of ϵ' and ϵ from Assumption [C](#).

Here, $J_n = J$, so Assumption 2 of [Shorack \(1972\)](#) is satisfied.

Finally, to show Assumption 3, we re-write the integral using integration by parts and

bound using Hölder's inequality as follows:

$$\begin{aligned}
& \int_0^1 M(t(1-t))^{-b+1/2-\epsilon/2} d|\mathbb{E}[\delta_i | Q_i = F_S^{-1}(t)]| \\
&= M(t(1-t))^{-b+1/2-\epsilon/2} |\mathbb{E}[\delta_i | Q_i = F_S^{-1}(t)]| \Big|_0^1 \\
&\quad - \int_0^1 M(t(1-t))^{-b-1/2-\epsilon/2} |\mathbb{E}[\delta_i | Q_i = F_S^{-1}(t)]| dt \\
&= M(t(1-t))^{-b+1/2-\epsilon/2} |\mathbb{E}[\delta_i | Q_i = F_S^{-1}(t)]| \Big|_0^1 \\
&\quad - \int_{-\infty}^{\infty} M(F_S(q)(1-F_S(q)))^{-b-1/2-\epsilon/2} |\mathbb{E}[\delta_i | Q_i = q]| dF_S(q),
\end{aligned}$$

where the last line follows from the change of variables $t = F_S(q)$. Recalling that because of the constraints on b in Assumption B, $b < 1/2$, and that Assumption C implies that

$$\sup_t |\mathbb{E}[\delta_i | Q_i = F_S^{-1}(t)]| < \infty,$$

the first term will be 0. The second term converges to zero because

$$\begin{aligned}
& \int_{-\infty}^{\infty} M(F_S(q)(1-F_S(q)))^{-b-1/2-\epsilon/2} |\mathbb{E}[\delta_i | Q_i = q]| dF_S(q) \\
&= \mathbb{E}[M(F_S(Q_i)(1-F_S(Q_i)))^{-b-1/2-\epsilon/2} |\mathbb{E}[\delta_i | Q_i]|] \\
&\leq \sqrt{\mathbb{E}[B^2(1-F_S(Q_i))(F_S(Q_i)(1-F_S(Q_i)))^\epsilon |\mathbb{E}[\delta_i | Q_i]|^2] \mathbb{E}[((1-F_S(Q_i))(F_S(Q_i)))^{-1+\epsilon}]} \\
&\leq \sqrt{C \mathbb{E}[B^2(1-F_S(Q_i))(F_S(Q_i)(1-F_S(Q_i)))^\epsilon \delta_i^2]} \rightarrow 0
\end{aligned}$$

for a constant $\mathbb{E}[((1-F_S(Q_i))(F_S(Q_i)))^{-1+\epsilon}] \leq C < \infty$ and by Assumption C to conclude that the last line goes to 0. Note that if $\epsilon' < \epsilon$ from Assumption C, the first term will involve an even larger exponent, and will still be bounded. \square

B Simulation Experiments: Power vs. HTE Strength and Power vs. Sample Size

We use several simulation experiments to probe aspects of RATE metrics' behavior, including

1. the power of the RATE in testing against a null hypothesis of no heterogeneous treatment effects. We consider this both as a function of sample size and as a function of the signal-to-noise ratio of the heterogeneous treatment effect function; and

We generate simulated data representing scenarios with both uncensored continuous and right-censored time-to-event/survival outcomes; employ several different kinds of prioritization rules, including CATE estimators like Causal Forests (Athey et al., 2019; Cui et al.,

2020), S-Learners, and X-Learners (Künzel et al., 2019), as well as risk estimators like traditional random forests (Breiman, 2001; Hastie et al., 2009); and consider both completely randomized trials as well as observational studies in which treatment assignment depends only on observable covariates (“unconfoundedness”). For the sake of illustration and brevity, we include in the main manuscript only one type continuous-outcome simulation and one type of survival-outcome simulation, each of which represents an observational study in the unconfoundedness setting.

B.1 Estimating RATEs in Observational Studies with Uncensored Outcomes and Unconfoundedness

One common context for estimating the RATEs is in studies with binary treatments, $W_i \in \{0, 1\}$, continuous and uncensored treatment outcomes, $Y_i \in \mathbb{R}$, and where we allow for treatment selection based on observable covariates by assuming that potential outcomes are conditionally independent of the treatment conditioned on observed subject data, $Y_i(1), Y_i(0) \perp\!\!\!\perp W_i | X_i$ (unconfoundedness).

B.1.1 Simulator Design

We start from the simulation “Setup A” in Nie and Wager (2017), in which data is generated as follows:

$$\begin{aligned} X_i &\sim \text{Unif}(0, 1)^d \\ e(X_i) &= \text{trim}_{0.1}\{\sin(\pi X_{i1} X_{i2})\} \\ W_i | X_i &\sim \text{Bernoulli}(e(X_i)) \\ b(X_i) &= \sin(\pi X_{i1} X_{i2}) + 2(X_{i3} - 0.5)^2 + X_{i4} + 0.5X_{i5} \end{aligned}$$

where $\text{trim}_\eta(x) = \max\{\eta, \min(x, 1 - \eta)\}$, X_i represents the model input features for the i^{th} subject, $e(\cdot)$ is the propensity function, W_i is a binary treatment indicator (1 if the i^{th} subject received treatment, 0 otherwise), and $b(\cdot)$ is the baseline main effect modeled after the scaled Friedman (1991) function. The treatment effect function, $\tau(\cdot)$, and observed outcome for the i^{th} subject, Y_i are:

$$\begin{aligned} \tau(X_i) &= (X_{i1} + X_{i2}) / 2 \\ \varepsilon_i | X_i &\sim \mathcal{N}(0, 1) \\ Y_i &= b(X_i) + (W_i - e(X_i))\tau(X_i) + \sigma_\varepsilon \varepsilon_i \end{aligned}$$

where σ_ε represents the strength of random noise in the observation model.

We modify this simulation slightly by (1) introducing a parameter σ_τ that controls the signal strength/variance of the heterogeneous treatment effects, and (2) replacing $\tau(X_i)$ with

$$\tilde{\tau}(X_i, \sigma_\tau) = \frac{\tau(X_i)}{SD(\tau)} \sigma_\tau,$$

where $SD(\tau) = \sqrt{\frac{1}{n-1} \sum_{i=1}^n (\tau(X_i) - \frac{1}{n} \sum_{i=1}^n \tau(X_i))^2}$.

We note that in this simulation, the nuisance parameters $e(\cdot)$ and $b(\cdot)$ are difficult to learn, but the treatment effect function is more straightforward.

B.1.2 Prioritization Rules

In the simulations, we study the RATE associated with prioritization rules generated as follows:

Oracle The Oracle prioritization rule assigns each subject a priority according to the true expected treatment effect conditioned on that subject's covariates. The Oracle thus has access to the true data generating process, though not the specific noise applied to each subject.

Random The Random prioritization rule assigns each subject a priority drawn uniformly at random from the interval $[0, 1]$. Note that a random prioritization rule will have a RATE of 0 for any weight function $\alpha(\cdot)$.

Random Forest (RF) Risk The RF Risk prioritization rule assigns each subject a priority in accordance with their estimated risk, where risk in this case is defined to be the subject's outcome in the absence of treatment: $\mu_0(x) = \mathbb{E}[Y_i(0)|X_i = x]$. We estimate the baseline risk using random forests, as implemented in `grf` (Athey et al., 2019). A key assumption in order for the RF Risk to achieve a high RATE is that risk is strongly correlated with the treatment effect. In our simulator setup, this is not the case.

Causal Forest The Causal Forest prioritization rule similarly uses ensembles of trees built with recursive partitioning to assign subject priorities but, unlike random forests, the causal forest chooses partitions

to minimize the CATE R-loss criterion (Nie and Wager, 2017). We use the Causal Forest implementation provided by `grf`.

X-learner Like the Causal Forest prioritization rule, the X-learner (Künzel et al., 2019) attempts to directly model the CATE as a function of patient covariates. However, the X-learner uses a different objective for targeting the CATE using the observed data. The algorithm is described with more detail by Künzel et al. (2019). We implement the X-learner with random forests (`grf`) as base model learners.

B.1.3 Estimating Doubly Robust Scores of the Treatment Effect

In this context, we estimate doubly robust scores for each participant using augmented inverse-propensity weighted (AIPW) scores, as described in equation (20). In these experiments, we use Random Forests (Breiman, 2001; Athey et al., 2019; Athey and Imbens, 2019) as implemented in `grf` to fit the propensity score, $\hat{e}(x)$, and marginal response curve, $\hat{m}(x, w)$, on folds in a cross-fit manner (Chernozhukov et al., 2018a).

B.2 Estimating RATEs with Continuous, Right-Censored Outcomes and Unconfoundedness

As discussed previously, a common context for validating prioritization rules with RATE metrics, especially in clinical studies with longitudinal outcomes, will be with time-to-event data with censoring.

B.2.1 Simulator Design

Adapting the “Second Scenario” in [Cui et al. \(2020\)](#), we generate covariates independently from a uniform distribution on $[0, 1]^5$. The propensity function $e(X_i)$ is generated from a Beta(2, 4) distribution, $e(X_i) = (1 + \beta(X_{i2}; 2, 4))/4$. The failure time, T_i , is generated from a proportional hazard model and the censoring time, C_i , from an accelerated failure time model as follows:

$$\begin{aligned} U_i &\sim \text{Uniform}(0, 1) \\ Z_i &\sim \mathcal{N}(0, 1) \\ T_i &= \left(\frac{-\log(U_i)}{\exp(X_{i1} + (-0.4 + X_{i2}) \cdot W_i)} \right)^2 \\ C_i &= \exp(X_{i1} - X_{i3} \cdot W_i + Z_i) \\ Y_i &= \min(T_i, C_i) \\ \Delta_i &= \mathbf{1}\{T_i \leq C_i\} \end{aligned}$$

Here Y_i represents the observed study time and Δ_i represents an indicator for right-censoring, as described previously.

B.2.2 Prioritization Rules

While our **Oracle** and **Random** prioritization rules remain the same as discussed in Section [B.1.2](#) for observational studies with unconfoundedness, we additionally analyzed three different prioritization rules adapted to the survival analysis setting.

Random Survival Forest (RSF) Risk Similar to the Random Forest (RF) Risk prioritization rule described previously, the Random Survival Forest (RSF) Risk prioritization rule estimates subjects’ outcomes in the absence of treatment using a collection of single tree models. As in traditional random forest models, these trees are constructed via bootstrap aggregating (“bagging”) and random variable selection to decide which variables to split and how, given the data ([Breiman, 2001](#)). Here, however, the outcome considered is the conditional survival function, $S(t, x) = P(Y_i(0) > t | X_i = x)$. Additionally, nodes within trees are split by choosing the variable and split point which maximize survival difference between child nodes ([Ishwaran et al., 2008](#)). We used survival forests as implemented in `grf` ([Athey et al., 2019](#)) to learn RSF prioritization rules.

Causal Survival Forest (CSF) The Causal Survival Forest (CSF) prioritization rule adapts the Causal Forest algorithm described in Section [B.1.2](#) to the setting of right-censored time-to-event outcomes. Concretely, given potential outcomes $T_i(1)$ and $T_i(0)$ representing survival times for the i^{th} subject under treatment and control arms, respectively, the CSF prioritization rule learns to estimate the restricted mean survival time, $\tau(x) = \mathbb{E} \left[\min\{T_i(1), t_0\} - \min\{T_i(0), t_0\} \mid X = x \right]$, from the data. This is accomplished by constructing an ensemble of single tree models, each of which directly targets heterogeneity in the CATE when determining how and where to split nodes. We use an implementation of Causal Survival Forests in `grf` ([Athey et al., 2019](#)) in our experiments.

Cox Proportional Hazards S-learner The Cox Proportional Hazards S-learner prioritization rule (CoxPH S-learner) adapts the canonical Cox Proportional Hazards survival model (Andersen and Gill, 1982) to the causal inference setting by (1) training a model to estimate the hazard ratio when treatment assignment is considered as simply an extra covariate in the model, $\hat{\lambda}(X_i = x, W_i = w)$; then (2) estimating the CATE on the test set as the difference for each individual between the model’s predictions if the subject were assigned to treatment and if they were assigned to control, i.e., $\hat{\tau}(x) = \hat{\lambda}(X_i = x, W_i = 1) - \hat{\lambda}(X_i = x, W_i = 0)$. In modeling $\hat{\lambda}$, we used an implementation of Cox Proportional Hazards provided within the `survival` package in R (Therneau and Grambsch, 2000). We included all covariates, treatment assignment, and first-order interaction terms between treatment assignment and the other covariates as predictors. This is a common practice for estimating heterogeneous treatment effects in clinical studies (Rekkas et al., 2020).

B.2.3 Estimating Doubly Robust Scores of the Treatment Effect

For the time-to-event setting, we use a doubly robust score defined in equation (22). For the sake of brevity we omit the exact formula and refer readers to Cui et al. (2020) for details. Note that in our experiments we estimate nuisance parameters, including the expected remaining survival time for each individual and the conditional survival function, using survival forests (Ishwaran et al., 2008) with cross-fitting, as implemented in the `grf` R package. Propensity score estimators are learned using random forests with cross-fitting, as also provided in the `grf` R package.

B.3 Analysis of Statistical Power

The statistical power of the hypothesis test described in Section 3.2 depends on both the strength of the heterogeneous treatment effects and the sample size. In the following subsections, we illustrate the relationship between statistical power and strength of heterogeneous treatment effects and the relationship between power and sample size, respectively. Then, we consider the effect that the weighting function of the RATE has on the power, for different distributions of heterogeneous treatment effects.

B.3.1 Power as a function of heterogeneous treatment effect strength

Using synthetic data from the simulator described in Section B.1.1, we learned nuisance parameter estimators and the prioritization rules described in Section B.1.2 on 1000 training samples and estimated the RATE on another 1000 i.i.d. test samples. For each prioritization rule, we calculated a P -value for $H_0 : \text{RATE} = 0$ using the procedure described in Section 3.2. We repeated this procedure 1000 times, and counted the fraction of simulations in which H_0 was rejected at significance level $\alpha = 0.05$ as a measure statistical power. This process of estimating power was repeated for a variety of heterogeneous treatment effect strengths σ_τ . When there was no heterogeneity in the treatment effects ($\sigma_\tau = 0$), the proportion of null hypotheses rejected was interpreted to be an estimate of the Type I error of our hypothesis test.

Results of this experiment can be seen in Figure 4. For prioritization rules that directly target the CATE (e.g., Causal Forests, X-learners), statistical power increased monotonically with heterogeneous treatment effect strength, as desired. We additionally observe that these two CATE-targeting estimators perform substantially better than a risk-based prioritization rule using random forests. This is to be expected given the simulator design.

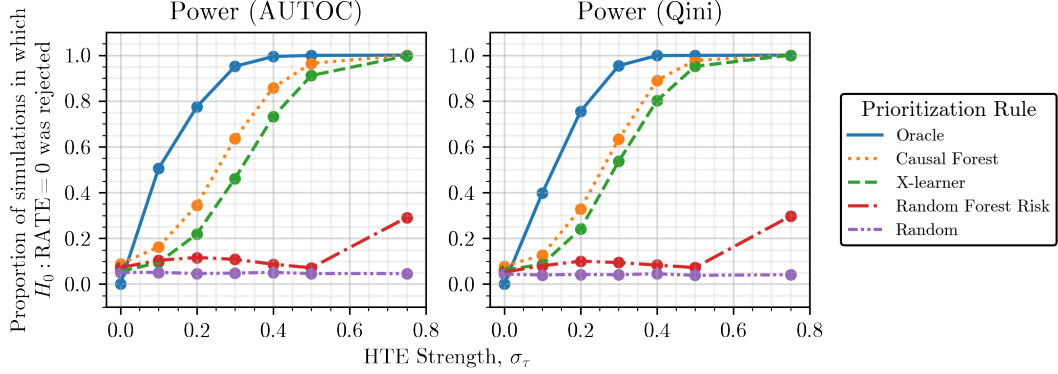


Figure 4. Power as a function of heterogeneous treatment effect strength, σ_τ , in Setup 1 for the RATE with both logarithmic (AUTOC) and linear (Qini) weighting. Of note, even when $\sigma_\tau = 0.3$ i.e. the variance/signal strength of the heterogeneous treatment effects was $\sigma_\tau^2/\sigma_\varepsilon^2 = 0.3^2 = 0.09 \approx 10\%$ that of the noise in the observed outcome model, we were able to use the procedure outlined in Section 3.2 to test against the presence of heterogeneous treatment effects with a power of > 0.6 and a Type I error of approximately 0.05. Once the signal-to-noise ratio approached closer to $\sigma_\tau^2/\sigma_\varepsilon^2 = 0.4^2 = 0.16$, we were able to test against the presence of heterogeneous treatment effects with a power of > 0.8 and a Type I error of 0.05 using the Causal Forest implemented in `grf` with default hyperparameters.

B.3.2 Power as a function of sample size

Using the simulator described in Section B.2.1, we estimated statistical power via the procedure outlined in the previous section. Here, however, instead of measuring power as a function of varying heterogeneous treatment effect strength, we analyzed how power changed with increasing sample size.

See Figure 5 for a summary of the results. Of note, the RATE increased monotonically with the sample size for prioritization rules that directly target the CATE (e.g., the Causal Survival Forest and Cox Proportional Hazards S-learner models). The same is not true of prioritization rules that only targeted risk/the baseline outcome (e.g., the Random Survival Forest Risk model).

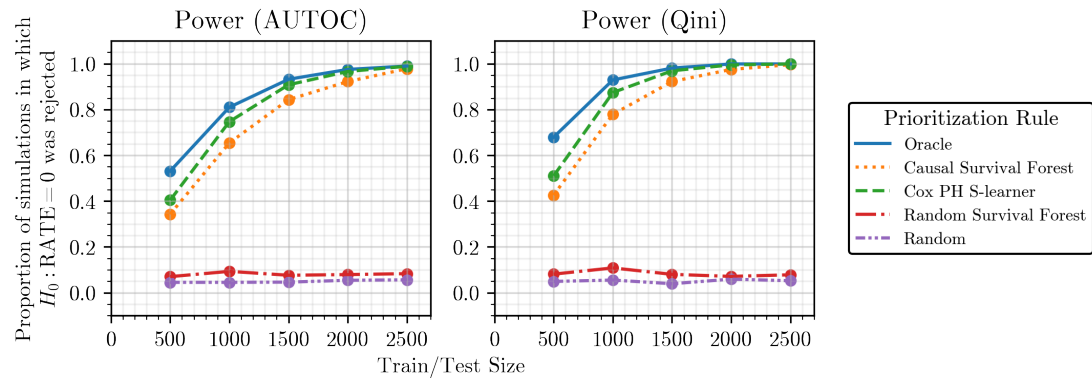


Figure 5. Statistical power in testing against the absence of heterogeneous treatment effects, as a function of sample size (train and test set size are identical within each simulation), in the context of right-censored, time-to-event outcomes under unconfoundedness.